TEXTURE ANALYSIS OF CT SCAN IMAGES

Thesis submitted in partial fulfillment of the requirement for the award of degree of

Master of Engineering

in

Electronic Instrumentation and Control

By:

Guneet Saini

(80651008)

Under the supervision of:

Mr. Mandeep Singh, Assistant Professor

&

Mr. M.D. Singh, Lecturer

ELECTRICAL AND INSTRUMENTATION DEPARTMENT

THAPAR UNIVERSITY,PATIALA

JUNE 2008

DECLARATION

The thesis submitted here is a study on texture analysis of abdominal CT scan images. I hereby declare that the report entitled "Texture Analysis of CT Scan Images" is an authentic record of my own work carried out as requirements for the award of degree of M.E. (Electronic Instrumentation & Control) at Thapar University, Patiala, under the supervision of Mr. Mandeep Singh, Assistant Professor and Mr. M.D. Singh, Lecturer, Electrical & Instrumentation Department, Thapar University, Patiala during January to June 2008.

(----------)
GUNEET SAINI
Roll No. 80651008

Date: 8 July 08

It is certified that the above statement made by the student is correct to the best of our knowledge and belief.

(----------)
Mr. M.D. Singh
Lecturer, EIED
Supervisor
Thapar University, Patiala

(---------- 08.07.08 ----------)
Mr. Mandeep Singh
Assistant Professor, EIED
Supervisor
Thapar University, Patiala

(----------)
Dr. Smarajit Ghosh
Professor & Head, EIED
Thapar University, Patiala

(----------)
Dr. R K Sharma
Dean of Academic Affairs
Thapar University, Patiala

ACKNOWLEDGEMENT

I would like to express my gratitude to all those who gave me the possibility to finish this thesis. I want to thank Electrical and Instrumentation Engineering Department of Thapar University for providing me the necessary software and other resources to deliver my research work.

I am deeply indebted to my advisors Mr. M.D. Singh, Lecturer and Mr. Mandeep Singh, Assistant Professor, Electrical & Instrumentation Department, for their help, encouragement, stimulating suggestions and guidance helped me all the time of research and writing of thesis.

I shall be failing in my duties if I do not express my deep sense of gratitude towards Dr. Smarajit Ghosh, Professor and Head of the Department of Electrical & Instrumentation Engineering, Thapar University, Patiala, who has been a constant source of inspiration for me throughout this work. I am also thankful to all the staff members of the Department for their full cooperation and help.

A special thanks to MRI radiology center, Chandigarh that played a great role in providing me with the CT scan images of abdomen. Without their help, this thesis would not have been possible.

Last but not the least: I owe my gratitude to the Almighty for giving me the courage and insight to complete this work. Especially, I would like to give my special thanks to my parents and family, for their patient love and encouragement enabled me to complete this work. My heartfelt thanks to all my colleagues and friendsfor thein help without which this work would not have been successful.

Place: Thapar University, Patiala
Date: 8 July/08

Guneet Saini

ABSTRACT

Medical imaging is though expensive because of capital costs, is easy to perform because of its noninvasive nature. It is clearly very important to extract the maximum possible information from any image obtained. However, image processing modes based on scan sections or radiographic views may not completely provide diagnostic information at an early stage, when it would be easier to control a disease, make a therapeutic decision, or perform surgery. This lack of timely information is, in part, because gray level differences in tissues are small compared to the accuracy with which the measurements may be carried out for a reasonable patient dose of X-rays. These limitations necessitate development of new analysis techniques that will improve diagnostic ability. One promising technique is texture analysis, which characterizes tissues to determine changes in functional characteristics of organs at the onset of disease.

In this study, we have tried to analyze the texture of Computed Tomography (CT) images taken of abdomen and to find the values of various parameters of texture. In the present study, we quantitatively establish the use of texture for detection of abnormalities in CT images that are beyond human appreciation and otherwise difficult to determine by other classical methods of image processing.

This study investigates whether the texture could be used to discriminate among the various tissue types in the abdomen CT scans and if so, what are the parameters which are useful for such an application. The present study focuses on contrast, homogeneity, energy, correlation, and entropy as parameters for texture.

ORGANIZATION OF THESIS

The first chapter is the introduction to feature extraction techniques and focuses on various methods of feature extraction. The second chapter is based on medical imaging, in which various medical imaging techniques are briefed and CT scan imaging process is discussed in detail. The next chapter deals with texture analysis methods and a detail study of the texture analysis method used in this thesis. The fourth chapter is based on the methodology used in this work. It gives the method used to complete this work. The last chapter concludes with the results and the conclusion with the future scope of the work.

TABLE OF CONTENTS

LIST OF FIGURES

LIST OF TABLES

LIST OF ABBREVIATIONS

CT SCAN - Computed Tomography Scan

GLCM - Gray Level Co occurrence Matrix

HU - Hounsfield

MATLAB - MATrix LABoratory

MRI - Magnetic Resonance Imaging

PET - Positron Emission Tomography

SPECT - Single Photon Emission Tomography

OCT - Optical Coherent Tomography

CHAPTER 1

INTRODUCTION

1.1 FEATURE EXTRACTION

In pattern recognition and in image processing, feature extraction is a special form of dimensionality reduction. When the input data to an algorithm is too large to be processed and it is suspected to be notoriously redundant (much data, but not much information) then the input data will be transformed into a reduced representation set of features. Transforming the input data into the set of features is called feature extraction. If the features extracted are carefully chosen it is expected that the feature set will extract the relevant information from the input data in order to perform the desired task using this reduced representation instead of the full size input. Features often contain information relative to gray shade, texture, shape, or context. To classify an object in an image, we must first extract some features out of the image. [http: Feature_extraction]

1.2 FEATURE EXTRACTION TYPES

Various techniques have been used to extract features from images. Some of the commonly used methods are discussed below.

1. Spatial features
2. Transform features
3. Edges & boundaries
4. Shape features
5. Moments
6. Texture

These are discussed in detail in following pages.

1.2.1 SPATIAL FEATURES

Spatial features of an object may be characterized by its gray levels, their amplitude features, spatial distribution etc.

1.2.1.2 AMPLITUDE FEATURES

The simplest and perhaps the most important features of an object are the amplitudes of the physical properties. For example in x-ray images, the gray level amplitude represents the absorption characteristics of the body masses & enables discrimination of bones from tissue or healthy tissue from diseased tissue.

1.2.1.2 HISTOGRAM FEATURES

The histogram of an image normally refers to a histogram of the pixel intensity values. This histogram is a graph showing the number of pixels in an image at each different intensity value found in that image. Figure 1.1 shows the histogram of an image. For an 8-bit grayscale image there are 256 different possible intensities, and so the histogram will graphically display 256 numbers showing the distribution of pixels amongst those grayscale values. Histograms can also be taken of color images - either individual histogram of red, green and blue channels can be taken, or a 3-D histogram can be produced, with the three axes representing the red, blue and green channels, and brightness at each point representing the pixel count.

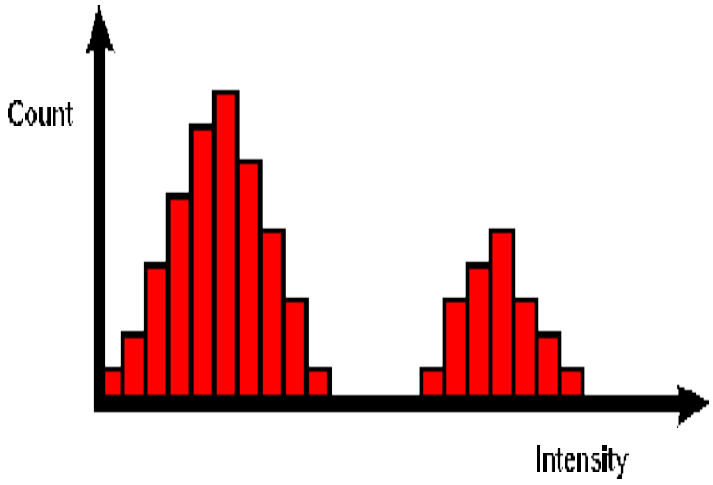

Figure 1.1 Histogram of an image

Some of the common histogram features are dispersion, mean, variance, mean square value or average energy, skewness, kurtosis. Other useful features are the median and the mode. A narrow histogram indicates a low contrast region. Variance can be used to measure local activity in the amplitudes.

1.2.2 TRANSFORM FEATURES

Image transforms provide the frequency domain information in the data. Transform features are extracted by zonal filtering the image in the selected transform space. The zonal filter, also called the feature mask, is simply a slit or an aperture. Generally the high frequency components can be used for boundary and edge detection, and angular slits can be used for detection of orientation.

Transform feature extraction techniques are also important when the source data originates in the transform coordinates.

1.2.3 EDGE DETECTION

Edges characterize object boundaries and are useful for segmentation, registration and identification of objects in scenes. Edge points can be thought of as

pixel locations of abrupt gray level change. For example, it is reasonable to define edge points in binary images as black pixels with at least one white nearest neighbor. The goal of edge detection is to mark the points in a digital image at which the luminous intensity changes sharply. Sharp changes in image properties usually reflect important events and changes in properties of the world. These include (i) discontinuities in depth, (ii) discontinuities in surface orientation, (iii) changes in material properties and (iv) variations in scene illumination. Edge detection of an image reduces significantly the amount of data and filters out information that may be regarded as less relevant, preserving the important structural properties of an image.

1.2.4 BOUNDARY EXTRACTION

Boundaries are linked edges that characterize the shape of an object. They are useful in computation of geometry features such as size or orientation. Different methods used are:

a) Connectivity

b) Contour Following

c) Edge Linking

a) CONNECTIVITY

Conceptually, boundaries can be found by tracing the connected edges. On a rectangular grid, a pixel is said to be four or eight-connected when it has the same properties as one it's nearest four or eight neighbors.

b) CONTOUR FOLLOWING

Contour following algorithms trace boundaries by ordering successive edge points. This algorithm can trace a boundary, open or closed, as a closed contour.

c) EDGE LINKING

A boundary can also be viewed as a path through a graph formed by linking the edge elements together. Linkage rules give the procedure for connecting the edge elements. Such features are useful because they frequently correspond to object or material boundaries, which are of interest. e.g., object recognition systems.

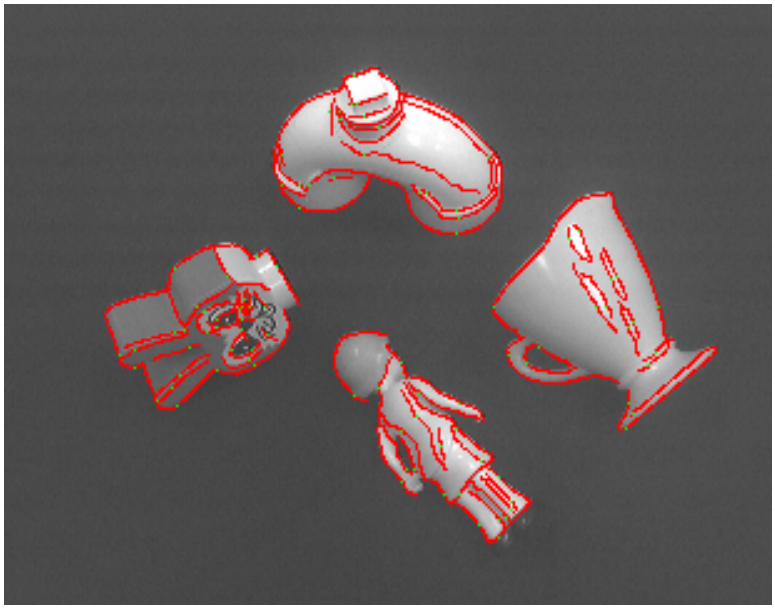

Figure 1.2 Edge Detection

1.2.5 SHAPE EXTRACTION

The shape of an object refers to its physical structure and profile. Example: Moments, perimeter, area, orientation etc. these characteristics can be represented by the previously discussed boundary, region, moment, and structural representations. These representations can be used for matching shapes, recognizing objects or for making measurement of shapes.

1.2.6 TEXTURE EXTRACTION

Texture is a combination of repeated patterns with a regular frequency. In visual interpretation texture has several types, for example, smooth, fine, coarse etc. Texture analysis is defined as the classification or segmentation of textural features with respect to the shape of a small element, density, and direction of regularity.

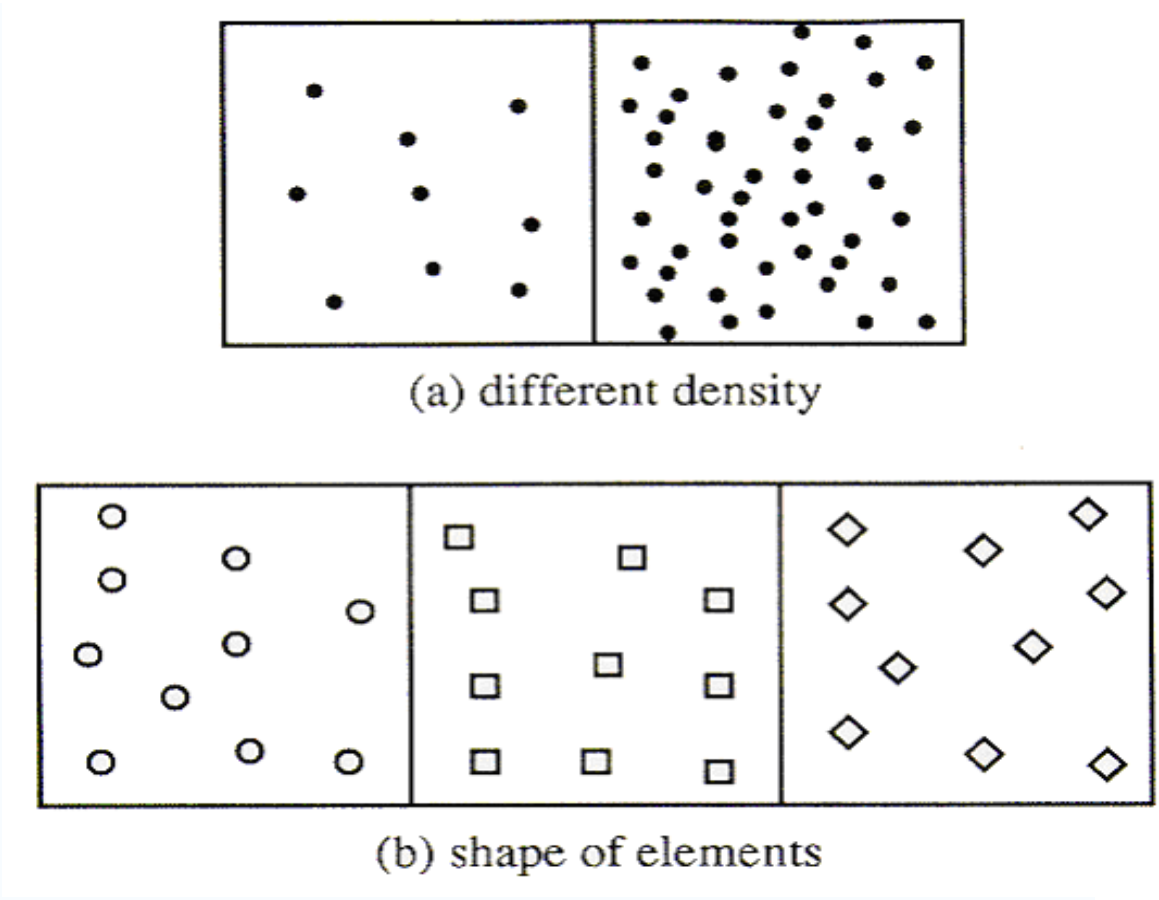

Figure 1.3 Texture Analysis

In the case of digital image, it is difficult to treat the texture mathematically because texture cannot be standardized quantitatively and the data volume is so huge. [http: texture]

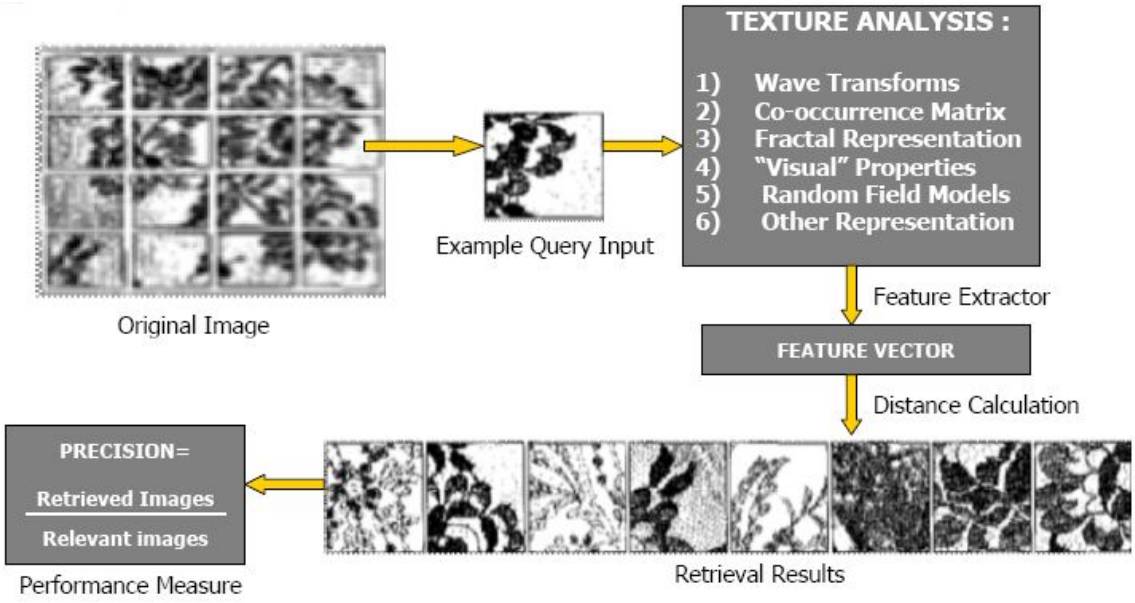

Figure 1.4 Texture Analysis Block Diagram

1.3 LITERATURE SURVEY

In 1973, Haralick et. al. proposed general procedure for extracting textural properties of blocks of image data. These features were calculated in the spatial domain, and the statistical nature of texture was taken into account in the procedure, which was based on the assumption that the texture information in an image I was contained in the overall or "average" spatial relationship which the gray tones in the image have to one another. They computed a set of gray tone spatial-dependence probability-distribution matrices for a given image block and suggested a set of 14 textural features, which can be extracted from each of these matrices. These features contained information about such image textural characteristics as homogeneity, gray-tone linear dependencies (linear structure), contrast, number and nature of boundaries present, and the complexity of the image. It was important to note that the number of operations required computing any one of these features was proportional to the number of resolution cells in the image block. It was for this reason that these features were called quickly computable. [Haralick et. al., 1973]

In 1988, John S. DaPonte et. al. proposed a method for choosing the direction of the displacement vector that was based on the most dominant edge obtained from gradient analysis. In addition, the anatomy of the liver was used to suggest the most important inter sample spacing in constructing co occurrence matrices for the evaluation of diffuse liver disease. For an inter sample spacing of 3 pixels, the most dominant edge was found to be 45" for the three normal cases and 135" for the case with fatty infiltration. Based on these preliminary results it was concluded that the gradient direction is more uniformly distributed in the fatty infiltration case then it was in the three normal cases. [DaPonte et. al., 1988]

In 1992, Chung-Ming W. et.al. studied the classification of ultrasonic liver images by making use of some powerful texture features, including the spatial gray-level dependence matrices, the Fourier power spectrum, the gray-level difference statistics, and the Laws' texture energy measures. In this paper, features of these types were used to

classify three sets of ultrasonic liver images-normal liver, hepatoma, and cirrhosis (30 samples each). [Chung-Ming, 1992]

In 1995, Mir A.H. et. al. in did some work in the use of texture for the extraction of diagnostic information from CT scan images. They obtained a number of features from abdominal ct scans of liver using the spatial domain texture analysis methods. This study investigated that whether texture could be used to discriminate between various tissue types that were inaccessible to human perception and if so, then what were the most useful parameters. The result was that the texture features were helpful in diagnosing the onset of disease in liver tissue, which cannot be done by visible eye. Three texture features namely - entropy, homogeneity, and gray level distribution were found to be effective. The performance of these features was compared on the basis of significance tests. The results showed that mainly all the parameters could detect the early malignancy with a confidence level of above 99%. [Mir et. al., 1995]

In 1996, Professor Yung-Nien Sun proposed a new ultrasonic image analysis system that could be utilized as an effective tool in classifying liver states as normal, hepatitis, or liver cirrhosis. In this system, first suitable settings for the ultrasonic device were defined, then the inhomogeneous structures from the area of interest were removed in the image, and then, by using the forward sequential search method, the useful texture parameters from the co-occurrence matrix, the statistical feature matrix, the texture spectrum, and the fractal dimension descriptors were looked. [Sun, 1996]

In 1996, S. Pavlopoulos et. al. attempted to determine the efficacy of computer assisted ultrasonic liver tissue characterization using texture analysis techniques. Two different algorithms were discussed in this study; the gray level difference statistics (GLDS) and the fractal dimension texture analysis (FDTA). Both techniques were applied on three sets of ultrasonic liver images, normal-hepatoma-cirrhosis. FDTA was able to differentiate cirrhosis and normal liver with an accuracy of 90 % and the GLDS was able to differentiate cirrhosis from normal with an accuracy of 75%. The combination of the two techniques proved to differentiate the three types with an overall accuracy of 81.7%. [Pavlopoulos et. al., 1996]

In 1996, E. Kyriacou et. al. evaluated the accuracy of image texture analysis techniques in the Characterization of ultrasonic liver images. The texture analysis techniques used were the Fractal Dimension Texture Analysis (FDTA), the Spatial Gray Level Dependence Matrices (SGLDM), the Gray Level Difference Statistics (GLDS), the Gray Level Run Length Statistics (RLJNL), and First Order gray level Parameters (FOP). The algorithms were applied on three sets of ultrasonic liver images, fatty, cirrhosis, normal, (30 samples each) all histological proven. The FDTA and SGLDM were able to characterize the three sets with accuracy of 80%, GLDS achieved 78.9% while RUNL and FOP both achieved 77.8% accuracy. Combination of GLDS and RUNI, gave 81.1%, while combination of FDTA and SGLDM gave 82.2% accuracy. [Kyriacou et. al., 1996]

In 2000, Qiang Ji et. al. described a texture image analysis technique for characterizing and recognizing typical, diagnostically most important, vascular patterns relating to cervical lesions. A generalized texture analysis technique was proposed based on combining the conventional statistical and structural approaches using a statistical description of geometric textural primitives. Preliminary experimental study demonstrated the feasibility of the proposed technique in discriminating between cervical texture patterns indicative of different stages of cervical lesions. [Ji Qiang et. al., 2000]

In 2001, Sharma M. et. al. used five different texture feature extraction methods that were most popularly used in image understanding studies. One of the features of this study was the use of a publicly available benchmark that further studies can use. Their results show that there was considerable performance variability between the various texture methods. Their finding, that co-occurrence matrices and Law's method perform better than other techniques, was supported by previous comparative studies in this area. It was however difficult to generalize this for all cases. The difference in results between the linear analysis and nearest neighbor method was also noteworthy. The best overall result using nearest neighbor methods was obtained with co-occurrence matrices, whereas using linear analysis the best result was obtained using combined set of features. It appears that since different texture methods capture different aspects of the image texture, and combining features from them has certainly much utility. [Sharma and Singh, 2001]

In 2001, Vassili A. Kovalev et. al. proposed a method for three-dimensional (3-D) texture analysis of magnetic resonance imaging brain datasets. The method was based on extended, multi sort co-occurrence matrices that combine intensity, gradient and anisotropy image features in a systematic and consistent way. They suggested co-occurrence descriptors are natively 3-D, reflection and translation invariant and, to some extent, rotation-insensitive. Normalization of co-occurrence descriptors provided a basis for inter subject analysis and comparisons of brain regions with different size. They showed that the extended co-occurrence descriptors could be used as an efficient tool in various MRI brain image analysis tasks such as classification of brain datasets and segmentation of diffuse brain lesions. [Kovalev et. al., 2001]

In 2002, Yi Wang et. al. used texture analysis with the co-occurrence matrix method to analyze ultra sonograms from normal and diseased livers, and X-ray CT images obtained from normal cases and cases of idiopathic interstitial pneumonia. Ten cases of normal, fatty, and cirrhotic livers; 10 cases of normal lungs; and 10 cases of idiopathic interstitial pneumonia, all confirmed by clinical findings, laboratory data, surgery, or biopsy, were the subjects of this study. In this paper, they compared the results of texture analysis in normal and diseased livers under the same conditions of gain, focus, magnification rate, probe frequency, and depth of the region of interest. They compared the results of texture analysis with images obtained from normal cases and cases of idiopathic interstitial pneumonia. Significant differences between normal lungs and those with idiopathic interstitial pneumonia were also found. Thus, it was concluded that texture analysis could be used to analyze ultra sonograms obtained from lesions of different pathological grades and to classify CT images as well. [Wang et. al., 2002]

In 2002, David A. Clausi studied the effect of grey level quantization on the ability of co-occurrence probability statistics to classify natural textures. None of the individual statistics showed increasing classification accuracy throughout all grey levels. Correlation analysis was used to rationalize a preferred subset of statistics. The preferred statistics set (contrast, correlation, and entropy) were demonstrated to be an improvement over using single statistics or using the entire set of statistics. Testing that compared (using all orientations separately), the average of all orientations and look direction

averaging, when determining the co-occurrence features, indicated that the look direction or all orientations was preferred. [Clausi, 2002]

In 2003, Joaquim Cezar Felipe et. al. proposed a study of supporting the retrieval and indexing of medical images by extracting and organizing intrinsic features of them, more specifically texture attributes from images. A tool for obtaining the relevant textures was implemented. This tool retrieved and classified images using the extracted values, and allowed the user to issue similarity queries. The application of the proposed method on images had given encouraging results that motivated to apply the method as a basis to more experiments, at diversified contexts. Two distinct experiments were performed: to determine the performance of different descriptors in the context of medical images; and to evaluate the precision vs. recall results for different tissue samples using the proposed method. The accuracy degree obtained from the precision and recall plots was always over 90% for queries asking for similar images for up to 20% of the database. [Felipe et. al., 2003]

In 2007, Mark A. Sheppard and Liwen Shih studied to double the accuracy of ultrasound diagnosis and biopsy guidance, an efficient, integrated platform for image textural analysis and clustering of transrectal prostate ultrasound images into clusters potentially representing cancerous or normal tissue areas. Preliminary image texture analysis showed the potential for doubling diagnosis accuracy from 38-42% for prostate cancer with current clinical methods, to 88-92%. In addition, image texture analysis made prostate cancer tumor locating possible for more precise, less invasive biopsy/treatment, instead of 6-way random biopsy. An efficient Image Texture Analysis tool platform on Window PC was constructed via innovative sparse co-occurrence matrix techniques with linked lists to speedup the processing from 8 days to about 5 seconds per image on a PC. The approach was based on Haralick's textural features and the Mean Squared Error (MSE) clustering algorithm. Ultrasound diagnosis was proven less invasive, even portable, at lower screening cost than most other medical imaging. However, being less visual than most, ultrasound image diagnosis was difficult even for trained professionals, and thus could benefit greatly from computer enhancement. [Sheppard and Liwen, 2007]

CHAPTER 2

MEDICAL IMAGING

2.1 INTRODUCTION

Medical imaging refers to the techniques and processes used to create images of the human body or parts for clinical purposes, that is, medical procedures seeking to reveal, diagnose or examine disease or medical science, including the study of normal anatomy and function. As a discipline and in its widest sense, it is part of biological imaging and incorporates radiology in the wider sense, radiological sciences, endoscopy, (medical) thermography, medical photography and microscopy (e.g. for human pathological investigations).

In the clinical context, medical imaging is generally equated to radiology or "clinical imaging". Diagnostic radiography designates the technical aspects of medical imaging and in particular the acquisition of medical images. The radiographer or radiologic technologist is usually responsible for acquiring medical images of diagnostic quality, although some radiological interventions are performed by radiologists. [http:Computed_tomography]

As a field of scientific investigation, medical imaging constitutes a sub-discipline of biomedical engineering, medical physics or medicine depending on the context. Research and development in the area of instrumentation, image acquisition (e.g. radiography), modelling and quantification are usually the preserve of biomedical engineering, medical physics and computer science. Research into the application and interpretation of medical images is usually the preserve of radiology and the medical sub-discipline relevant to medical condition or area of medical science (neuroscience, cardiology, psychiatry, psychology, etc) under investigation. Many of the techniques developed for medical imaging also have scientific and industrial applications.

Images of the human body are derived from the interaction of energy with human tissue. The energy can be in the form of radiation, magnetic or electric fields, or acoustic energy. The energy usually interacts at the molecular or atomic levels, so a clear understanding of the structure of the atom is necessary. [http: radiology]

In addition to understanding the physics of the atom, learning imaging jargon is also necessary. For example:

1. Tomography: A cross-sectional image formed from a set of projection images. The Greek word tomo means cut.
2. CT: Computed (or Computerized) Tomography
3. MR or MRI: Magnetic Resonance Imaging. This was first called nuclear magnetic resonance (NMR), but the mention of anything nuclear scared patients, so the "N" was dropped.
4. PET: Positron Emission Tomography. Understanding this phenomenon requires acceptance of the theory that there is antimatter in the universe, and when antimatter meets matter, then both kinds of matter are annihilated, and pure energy is formed.
5. SPECT: Single Photon Emission Tomography
6. Ultrasound: Sonar in the body
7. OCT: Optical Coherent Tomography – the use of infrared light to image (particularity) the walls of an artery.

A comparison of various techniques used in medical imaging in shown in Table 2.1.

Table 2.1 Comparison of Medical imaging Techniques

METHOD	PARAMETER MEASURED	MEDICAL APPLICATIONS
Transmission computed tomography	Density and average atomic number	Anatomy, mineral content, flow from movement of contrast material
Emission computed tomography	Concentration of radio nuclides	Metabolism, receptor site concentration, flow
Magnetic resonance	Concentrations, relaxation parameters and frequency shifts due to chemical form	Anatomy, edema, flow, chemical composition
Ultrasound	Acoustic impedance mismatch, sound velocity, attenuation, frequency shifts due to motion	Anatomy, tissue structure characteristics, flow

2.2 COMPUTED TOMOGRAPHY

Computed Tomography (CT) is a medical imaging method employing tomography. Digital geometry processing is used to generate a three-dimensional image of the inside of an object from a large series of two-dimensional X-ray images taken around a single axis of rotation. [http: history]

Computed tomography is probably the most common source of 3 dimensional data. CT scanners are relatively inexpensive, and most hospitals have at least one scanner. CT uses an X-ray radiation source to image the patient.

2.2.1 WORKING OF CT SCANNER

The CT scanner consists of a couch upon which the patient is placed and a circular gantry through which the couch with patient is passed. Within the gantry is a rotating ring with an X-ray source opposed to a linear array of detectors. A typical CT scan machine is shown in Figure 2.1*.

The X-ray source is collimated so that the X-rays form a flat fan beam with a thickness determined by the user. During the acquisition of a "slice" of data, the source-detector ring is rotated around the patient. The raw output from the detector array is back projected to form an image of the slice of the body. The couch is moved and then another slice is obtained.

Figure 2.1 CT Scan Machine- A Philips 64 slice 'Brilliance' Scanner

**http://en.wikipedia.org/wiki/Image:64_slice_scanner.JPG*

The output from a CT scanner is a series of trans axial slices of the patient. Each slice represents a slab of the patients' body with a thickness set by the collimation for the slice (typically 1-10mm). For most CT scanners each slab has 512 by 512 pixels. The size of a pixel can be varied within certain limits (generally 0.5 to 2 mm). Generally each slice is spaced such that they are either overlapping or contiguous, though some protocols call for gaps between the slices. Each pixel ideally represents the absorption characteristics of the small volume. Modern CT scanners can generally acquire one slice within 1 to 5 seconds. An entire study of a patient generally represents 30-40 slices, with a study time of 3-15 minutes. The radiation dose from a CT scan is comparable with that of a series of traditional X-rays. This is measured in Hounsfield units (HU).

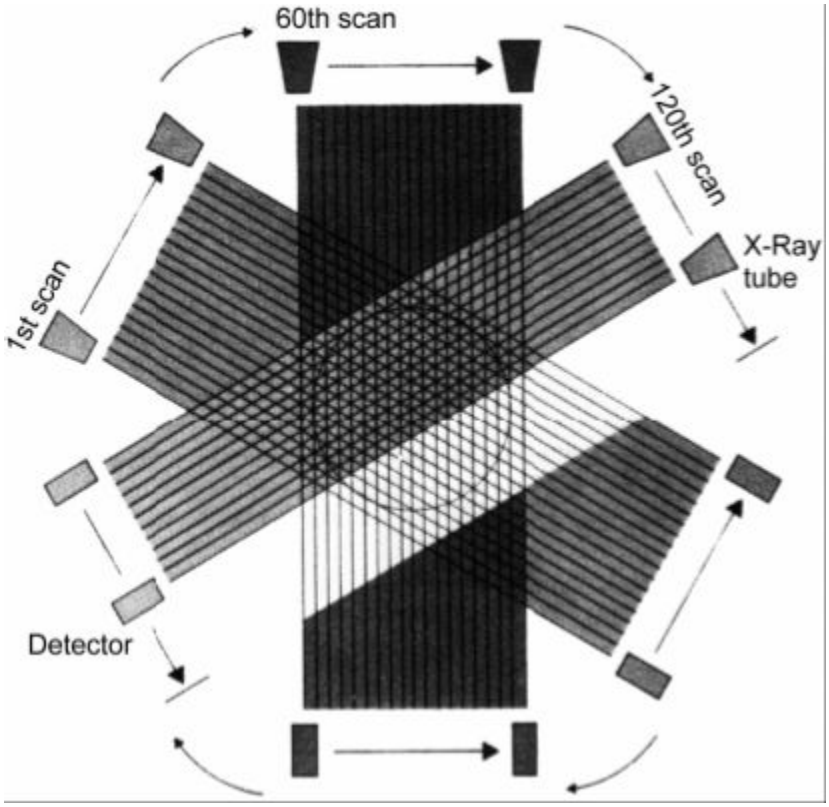

Figure 2.2 Various Scans at Different Angles

X-ray slice data is generated using an X-ray source that rotates around the object; X-ray sensors are positioned on the opposite side of the circle from the X-ray source. Figure 2.2 shows various scans at different angles.

The earliest sensors were scintillation detectors, with photomultiplier tubes excited by (typically) sodium iodide crystals. Modern detectors use the ionization principle and are filled with low-pressure Xenon gas. Many data scans are progressively taken as the object is gradually passed through the gantry. CT produces a volume of data which can be manipulated, through a process known as windowing, in order to demonstrate various structures based on their ability to block the X-ray beam. Although historically the images generated were in the axial or transverse plane (orthogonal to the long axis of the body), modern scanners allow this volume of data to be reformatted in various planes or even as volumetric (3D) representations of structures. [http: ct]

A CT scanner uses a series of X-ray beams to build up images of the body in slices. Unlike an X-ray, which sends one beam of radiation through the body, a CT scanner emits a succession of narrow beams as it moves through an arc. This produces a very detailed image that is not possible from a normal X-ray.

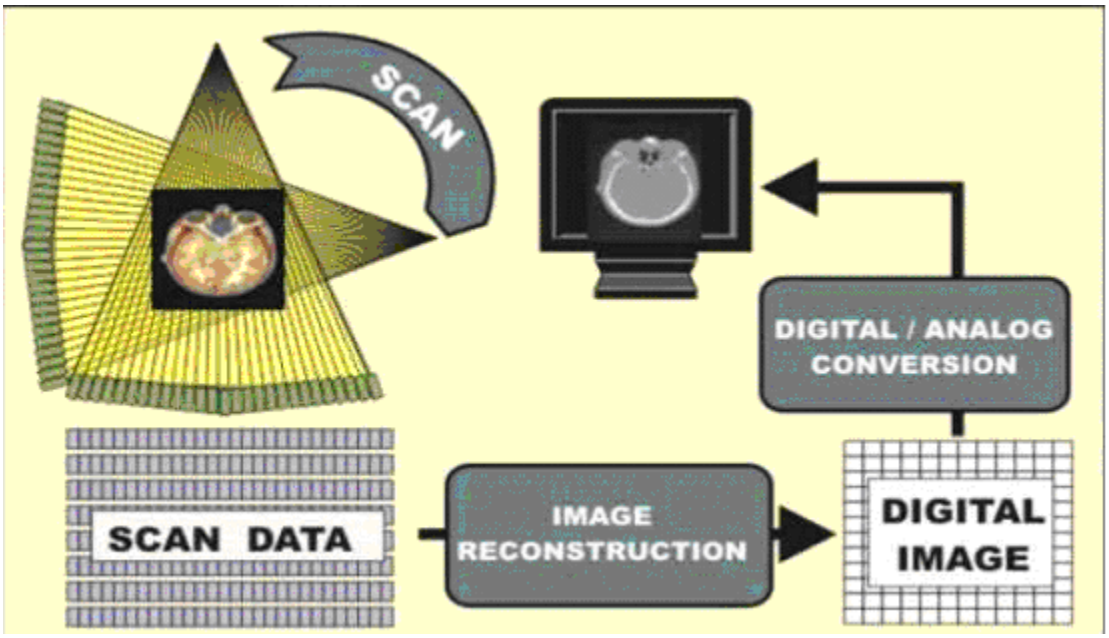

Figure 2.3 Conversion of Scanned Data into Medical Image

The X-ray detector within a CT scanner can see hundreds of different levels of density, including tissues within solid organs such as the liver. This information is then

sent to a computer, which builds up a cross-sectional image of the body and displays it on the screen. Figure 2.3 sums up the steps taken to form an image from scanned data.

Depending on the part of the body being examined, a contrast dye may be used to make some tissues show up more clearly under X-ray. For scans of the abdomen, you might be given a drink containing barium. This is known as a barium meal, and shows up white on the scans as it moves through the digestive tract. Contrast dyes may also be given as an enema or injected into the blood stream, depending on the part of your body that is to be scanned. 2D & 3D imaging is achieved by rotating an x-ray emitter around the patient, and measuring the intensity of transmitted rays from different angles.

A relatively new technique, a spiral CT has improved the speed and accuracy of the scan for many diseases. The X-ray beam takes a continuous spiral path during scanning, gathering continuous data with no gaps between images. A spiral scan can usually be obtained while holding your breath, which allows a scan of the chest to be done in a few seconds.

2.3 ABDOMINAL AND PELVIC CT SCAN

CT is a sensitive method for diagnosis of abdominal diseases. It is used frequently to determine stage of cancer and to follow progress. It is also a useful test to investigate acute abdominal pain (especially of the lower quadrants, whereas ultrasound is the preferred first line investigation for right upper quadrant pain). Renal stones, appendicitis, pancreatitis, diverticulitis, abdominal aortic aneurysm, and bowel obstruction are conditions that are readily diagnosed and assessed with CT. CT is also the first choice for detecting solid organ injury after trauma. It may be part of abdominal scanning (e.g. for tumors), and has uses in assessing fractures. Abdominal CT scans are used to detect tumors and to diagnose conditions in which internal organs, including the liver, kidneys, pancreas, intestines, and lungs are enlarged. The Figure 2.4 shows the abdominal CT scan procedure.

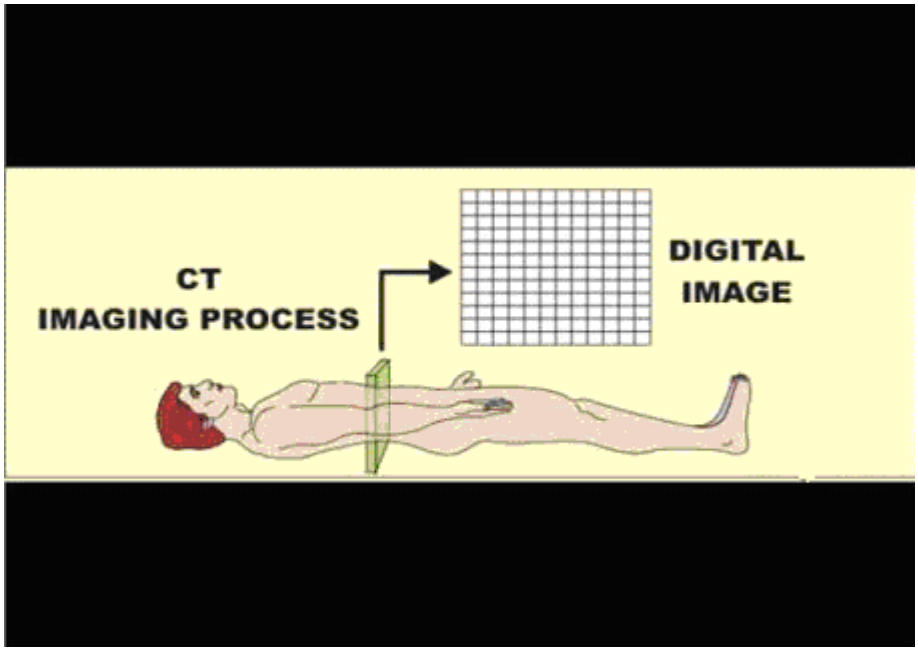

Figure 2.4 Abdominal CT Scan

Tears (lacerations) of the spleen, kidneys, or liver, which may occur in serious road traffic accidents, can be revealed by CT scan. An abdominal CT rapidly creates detailed pictures of the belly area. The test may be used to:

1) Study blood vessels

2) Identify masses and tumors, including cancer

3) Look for infections, kidney stones, or appendicitis

2.4 ADVANTAGES OF CT SCANS

CT completely eliminates the superimposition of images of structures outside the area of interest. Because of the inherent high-contrast resolution of CT, differences between tissues that differ in physical density by less than 1% can be distinguished. Data from a single CT imaging procedure consisting of either multiple contiguous or one helical scan can be viewed as images in the axial, coronal, or sagittal planes, depending on the diagnostic task. This is referred to as multiplanar reformatted imaging.

The improved resolution of CT has permitted the development of new investigations, which may have advantages. Compared to conventional angiography for example, CT angiography avoids the invasive insertion of an arterial catheter and guidewire; CT colonography may be as useful as a barium enema for detection of tumors, but may use a lower radiation dose. By viewing a CT scan, an experienced radiologist can diagnose many causes of abdominal pain with very high accuracy, enabling faster treatment and often eliminating the need for additional, more invasive diagnostic procedures.

When pain is caused by infection and inflammation, the speed, ease and accuracy of a CT examination can reduce the risk of serious complications caused by a burst appendix or ruptured diverticulum's and the subsequent spread of infection.

CT scanning is painless, noninvasive and accurate. A major advantage of CT is that it is able to image bone, soft tissue and blood vessels all at the same time. Unlike conventional x-rays, CT scanning provides very detailed images of many types of tissue as well as the lungs, bones, and blood vessels. CT examinations are fast and simple; in emergency cases, they can reveal internal injuries and bleeding quickly enough to help save lives.

CT has been shown to be a cost-effective imaging tool for a wide range of clinical problems. CT may be less expensive than MRI. In addition, it is less sensitive to patient movement. CT can be performed if you have an implanted medical device of any kind, unlike MRI. CT imaging provides real-time imaging, making it a good tool for guiding minimally invasive procedures such as needle biopsies and needle aspirations of many areas of the body, particularly the lungs, abdomen, pelvis and bones. A diagnosis determined by CT scanning may eliminate the need for exploratory surgery and surgical biopsy. No radiation remains in a patient's body after a CT examination. X-rays used in CT scans usually have no side effects. [http: advantages]

2.5 HAZARDS OF CT SCANS

CT is regarded as a moderate to high radiation diagnostic technique. While technical advances have improved radiation efficiency, there has been simultaneous pressure to obtain higher-resolution imaging and use more complex scan techniques, both of which require higher doses of radiation. The radiation from current CT-scan use may cause as many as 1 in 50 future cases of cancer. Pregnant women should not have a CT scan, as there is a small risk that X-rays may cause an abnormality to the unborn child. Nursing mothers should wait for 24 hours after contrast material injection before resuming breast-feeding.

The contrast dye used in CT scans often contains iodine, which can cause an allergic reaction in a few people. Very rarely the dye may cause some kidney damage in people who already have kidney problems. There is always a slight chance of cancer from radiation. However, the benefit of an accurate diagnosis far outweighs the risk. Children should have a CT study only if it is essential for making a diagnosis and should not have repeated CT studies unless absolutely necessary.

A person who is very obese may not fit into the opening of a conventional CT unit. CT Scanning of the abdomen may not be as sensitive in identifying gallstones as ultrasound of the abdomen. For some conditions, including but not limited to some liver, adrenal and pancreatic abnormalities, the evaluation and diagnosis with MRI may be preferable over CT scanning.

CHAPTER 3

TEXTURE ANALYSIS

3.1 TEXTURE ANALYSIS

Texture is an important characteristic for the analysis of many types of images. It can be seen in all images from multi spectral scanner images obtained from aircraft or satellite platforms (which the remote sensing community analyzes) to microscopic images of cell cultures or tissue samples (which the biomedical community analyzes). Despite its importance and ubiquity in image data, a formal approach or precise definition of texture does not exist. The texture discrimination techniques are, for the most part, ad hoc.

Image texture, defined as a function of the spatial variation in pixel intensities (gray values), is useful in a variety of applications and has been a subject of intense study by many researchers. One immediate application of image texture is the recognition of image regions using texture properties. Texture is the most important visual cue in identifying these types of homogeneous regions. This is called texture classification.

Image analysis techniques have played an important role in several medical applications. In general, the applications involve the automatic extraction of features from the image which is then used for a variety of classification tasks, such as distinguishing normal tissue from abnormal tissue. Depending upon the particular classification task, the extracted features capture morphological properties, color properties, or certain textural properties of the image. [http: texture]

Texture is a combination of repeated patterns with a regular frequency. In visual interpretation texture has several types, for example, smooth, fine, coarse etc., which are often used in the classification of forest types. Texture analysis is defined as the classification or segmentation of textural features with respect to the shape of a small element, density and direction of regularity. In the case of digital image, it is difficult to

treat the texture mathematically because texture cannot be standardized quantitatively and the data volume is so huge. [http: texture-review]

3.2 TEXTURE ANALYSIS TYPES

Approaches to texture analysis are usually categorized into:

1. Structural,
2. Statistical,
3. Model-based and
4. Transform

3.2.1 STRUCTURAL APPROACH

Structural approaches represent texture by well defined primitives (micro texture) and a hierarchy of spatial arrangements (macro texture) of those primitives. To describe the texture, one must define the primitives and the placement rules. The choice of a primitive (from a set of primitives) and the probability of the chosen primitive to be placed at a particular location can be a function of location or the primitives near the location. [Haralick, 1979]

The advantage of the structural approach is that it provides a good symbolic description of the image; however, this feature is more useful for synthesis than analysis tasks. The abstract descriptions can be ill defined for natural textures because of the variability of both micro- and macrostructure and no clear distinction between them.

3.2.2 STATISTICAL APPROACH

In contrast to structural methods, statistical approaches do not attempt to understand explicitly the hierarchical structure of the texture. Instead, they represent the texture indirectly by the non-deterministic properties that govern the distributions and relationships between the grey levels of an image. Methods based on second-order

statistics (i.e. statistics given by pairs of pixels) have been shown to achieve higher discrimination rates than the power spectrum (transform-based) and structural methods. Accordingly, the textures in grey-level images are discriminated spontaneously only if they differ in second order moments. Equal second order moments, but different third-order moments require deliberate cognitive effort.

The statistical approach exploits the statistical properties of image or image regions in a bottom up fashion, starting from the pixel values in the neighborhood. The co-occurrence matrix is in wide use in representing the dependence in the distributions of gray-level [Haralick, 1973]. The co-occurrence matrix is a function of: 1) the image region, 2) a displacement vector d = (dx, dy), and 3) the number of gray-levels after quantization. The matrix contains frequencies of co-occurrence of two gray-levels. After normalization, it becomes a probability matrix with all the elements summing up to 1.

3.2.3 MODEL BASED APPROACH

Model based texture analysis using fractal and stochastic models, attempt to interpret an image texture by use of, respectively, generative image model and stochastic model. The parameters of the model are estimated and then used for image analysis. In practice, the computational complexity arising in the estimation of stochastic model parameters is the primary problem. The fractal model has been shown to be useful for modeling some natural textures. It can be used also for texture analysis and discrimination; however, it lacks orientation selectivity and is not suitable for describing local image structures.

3.2.4 TRANSFORM BASED APPROACH

Transform methods of texture analysis, such as Fourier and wavelet transforms represent an image in a space whose co-ordinate system has an interpretation that is closely related to the characteristics of a texture (such as frequency or size). Methods based on the Fourier transform perform poorly in practice, due to its lack of spatial localization. Gabor filters provide means for better spatial localization; however, their

usefulness is limited in practice because there is usually no single filter resolution at which one can localize a spatial structure in natural textures.

3.3 APPROACH USED - STATISTICAL METHODS

The evaluation and development of new approaches for calculating texture have been a particular focus. Historically there have been two major approaches, i.e., structural and statistical approaches. The structural approach describes a texture by a sub pattern or primitive and spatial distribution of primitives, so called the placement rule. The primitives are also called texture elements. For instance, to consider the brick wall the primitive is a brick and the placement rule specifies the arrangement of bricks in the wall.

The statistical approach does not presume in term of primitive but it draws on the general set of statistical tool. It is the most widely used and more generally applied method because of its high accuracy and less computation time.

Texture statistics is frequently classified into first-order, second-order and high-order statistics. They are referring to the gray level distribution of pixel on an image. The gray scale is a black and white image at any given focus of pixel, typically there is a corresponding intensity on a range from 0 (black) to 255(white). That means an image is composed of an array of pixels of varying intensity across the image, the intensity corresponding to the level of grayness from black (0) to white (255) at any particular point in the image.

3.3.1 GRAY-LEVEL CO-OCCURRENCE MATRICES

The gray-level co-occurrence matrix (GLCM), a frequency matrix, is a useful method for enhancing details and is frequently used as an aid for interpretation of an image. The GLCM is a tabulation of how often different combinations of pixel brightness values (grey levels) occur in an image. The GLCM indicates the frequency of a pair of pixels that are at “exactly the same distance and direction of the displacement vector”. From this principal, it uses to computes the relationships of pixel intensity to the intensity of its neighboring pixels which are based on hypothesis that the same gray level

configuration is repeated in a texture and pixels that are close together tend to be more related than pixels that are far away from each other.

GLCM was introduced by Haralick in 1979 and some authors, Carstensen (2002); Cooper (2004); Basset (2000); Barber et al., 1993 and Lefebvre et al., 2000. They had suggested that the GLCM could describe the probability of finding pixels of gray level value i and j at a given displacement h.

The GLCM, c, is defined with respect to given (row, column) displacement h. And element (i , j), denoted c_{ij}, is the number of times a point having gray level j occurs in position h relative to a point having gray level i. Let Nh be the total number of pairs, then $C_{ij} = c_{ij} /Nh$ is the elements of the normalized GLCM, C.

Graycomatrix creates the GLCM by calculating how often a pixel with gray-level (grayscale intensity) value i occurs horizontally adjacent to a pixel with the value j. Each element (i,j) in glcm specifies the number of times that the pixel with value i occurred horizontally adjacent to a pixel with value j.

The co-occurrence probabilities provide a second-order method for generating texture features. These probabilities represent the conditional joint probabilities of all pair wise combinations of grey levels in the spatial window of interest given two parameters: inter pixel distance (δ) and orientation (θ). The probability measure can be defined as:

$$\Pr(x) = \{C_{ij} \mid (\delta, \theta) \}$$

Where Cij (the co-occurrence probability between grey levels i and j) is defined as:

$$Cij = \frac{Pij}{\sum_{i,j=1}^{G} Pij}$$

Where P_{ij} represents the number of occurrences of grey levels i and j within the given window, given a certain (δ, θ) pair;

G is the quantized number of grey levels.

The sum in the denominator thus represents the total number of grey level pairs (i, j) within the window.

Graycomatrix calculates the GLCM from a scaled version of the image. By default, if I is a binary image, graycomatrix scales the image to two gray-levels. If I is an intensity image, graycomatrix scales the image to eight gray-levels.

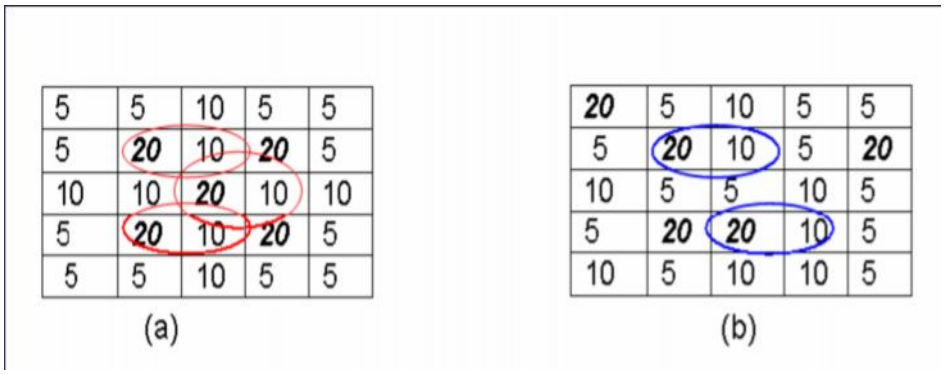

5	5	10	5	5
5	**20**	10	**20**	5
10	10	**20**	10	10
5	**20**	10	**20**	5
5	5	10	5	5

(a)

20	5	10	5	5
5	**20**	10	5	**20**
10	5	5	10	5
5	**20**	**20**	10	5
10	5	10	10	5

(b)

Figure 3.1 Example matrix for GLCM

If h= (0, 1), i.e., one step in the horizontal direction, then c (GLCM) will be

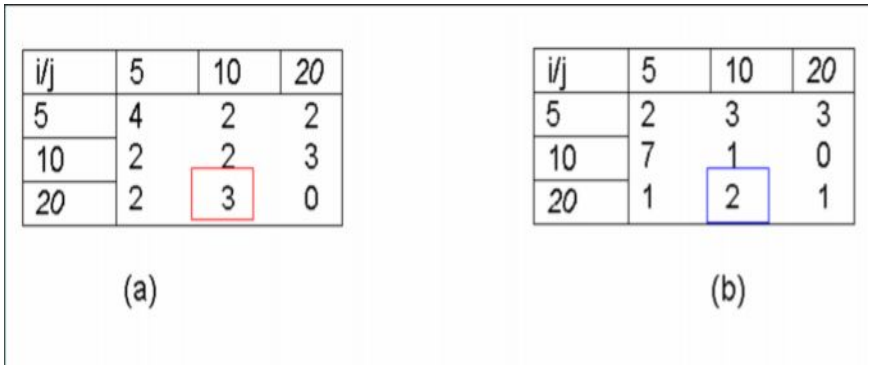

i/j	5	10	20
5	4	2	2
10	2	2	3
20	2	3	0

(a)

i/j	5	10	20
5	2	3	3
10	7	1	0
20	1	2	1

(b)

Figure 3.2 GLCM of the Matrix

The position of each element in the matrix indicates which pixel values are being compared (Figure3.1). The value at row i and column j gives the number of times that a pixel with the value j was to the immediate right of a pixel with the value i. Hence, the

value 3 in the 2nd column, 3rd row of Figure 3.2 indicates that a pixel value of 10 was to the right of a pixel with the value 20 counted 3 times. Meanwhile, the value 2 in the same position of GLCM from Figure 3.2 means a pixel value of 10 was to the right of a pixel with the value 20 counted 2 times.

GLCM texture considers the relation between two pixels at a time, called the reference and the neighbor pixel. In the illustration, the neighbor pixel is chosen to be the one to the east (right) of each reference pixel. This can also be expressed as a (1,0) relation: 1 pixel in the x direction, 0 pixels in the y direction.

Each pixel within the window becomes the reference pixel in turn, starting in the upper left corner and proceeding to the lower right. Pixels along the right edge have no right hand neighbor, so they are not used for this count.

3.3.2 FORMING THE MATRIX FRAMEWORK

The top left cell is filled with the number of times the combination 0,0 occurs, i.e. how many times within the image area a pixel with grey level 0 (neighbor pixel) falls to the right of another pixel with grey level 0 (reference pixel).

3.3.3 CREATING A TEXTURE IMAGE

The result of a texture calculation is a single number representing the entire window. This number is put in the place of the centre pixel of the window, then the window is moved one pixel and the process is repeated of calculating a new GLCM and a new texture measure. In this way an entire image is built up of texture values.

3.3.4 CALCULATING TEXTURE MEASURES FROM THE GLCM

Haralick defined a large number of features based on co-occurrence matrices, such as contrast, homogeneity, correlation, energy and entropy. [Haralick, 1973]
These features are briefly discussed in this section.

3.3.4.1 CONTRAST

Contrast is also called "sum of squares variance. Spatial frequency is the difference between the highest and the lowest values of a contiguous set of pixels. This definition holds for the GLCM contrast expression as well, in particular when the module of the displacement vector is equal to one. This implies that a low contrast image is not necessarily characterized by a narrow gray level distribution, i.e., it does not necessarily present a low variance value, but the low contrast image certainly features low spatial frequencies. The conclusion is that the GLCM contrast tends to be highly correlated with spatial frequencies while the module of the displacement vector tends to one. With regard to the GLCM variance and contrast pair, the only condition that relates these two parameters to each other is the following: a sufficient, but not necessary, condition to keep contrast low is to maintain variance low (while the vice versa is not true). A low contrast image presents a GLCM concentration term around the principal diagonal and, consequently, a low value of the GLCM contrast. This result means that high contrast values imply high contrast texture, first-order statistics contrast and GLCM contrast are strongly related. GLCM contrast and variance were also found to be highly correlated with the first order statistic standard deviation, but this condition, according to the Theoretical discussion presented above, must be considered as a particular case for the contrast parameter.

Mathematically, contrast can be represented as:

$$\sum_{i,j} | i - j |^2 P(i, j)$$

When i and j are equal, the cell is on the diagonal and (i-j) = 0. These values represent pixels entirely similar to their neighbor, so they are given a weight of 0. If i and j differ by 1, there is a small contrast, and the weight is 1. If i and j differ by 2, contrast is increasing and the weight is 4. The weights continue to increase exponentially as (i-j) increases.

3.3.4.2 HOMOGENEITY

Homogeneity is also called the "Inverse Difference Moment". Mathematically, it can be written as:

$$\sum_{i,j} \frac{P(i,j)}{1+|i-j|}$$

This parameter is also called Uniformity.

3.3.4.3 CORRELATION

GLCM correlation is expressed by the correlation coefficient between two random variables i and j , where i represents the possible outcomes in gray tone measurement for the first element of the displacement vector, while similarly j is associated with gray tones of the second element of the displacement vector. Its mathematical formula is given below:

$$\sum_{i,j} \frac{(i-\mu i)(j-\mu j)P(i,j)}{\sigma_i \sigma_j}$$

Correlation is a measure of gray tone linear-dependencies in the image; in particular, the direction under investigation is the same as vector displacement. High correlation values (close to 1) imply a linear relationship between the gray levels of pixel pairs. Thus, GLCM correlation is uncorrelated with GLCM energy and entropy, i.e., to pixel pairs repetitions. Correlation reaches it maximum regardless of pixel pair occurrence, as high correlation can be measured either in low or in high energy situations. GLCM correlation is also uncorrelated to GLCM contrast, as high predictability of the gray level of one pixel from the second one in a pixel pair is completely independent

from contrast. As a limiting case of linear-dependency a completely homogeneous area may be considered, for which correlation is equal to 1.

3.3.4.4 ENERGY

The mathematical formula for energy is given as:

$$\sum_{i,j} P(i,j)^2$$

Energy measures textural uniformity, i.e., pixel pairs repetitions; when the image patch under consideration is homogeneous (only similar gray level pixels are present) or when it is texturally uniform (the vector displacement always falls on the same (2, j) gray level pair). A few (possibly only one) elements of GLCM will be greater than 0 and close to 1, while many elements will be close to 0. In this case, energy reaches values close to its maximum, equal to 1. Thus, high energy values occur when the gray level distribution over the window has either a constant or a periodic form. This result means that energy is strongly uncorrelated to first order statistical variables such as contrast and variance. Indeed, energy may reach its maximum with either maximum or no variance and contrast values. Energy is the opposite of entropy. Energy can be used to do useful work. In that sense, it represents orderliness. This is why "Energy" is used for the texture that measures order in the image.

3.3.4.5 ENTROPY

Entropy is a notoriously difficult term to understand; the concept comes from thermodynamics. It refers to the quantity of energy that is permanently lost to heat ("chaos") every time a reaction or a physical transformation occurs. Entropy cannot be recovered to do useful work. Because of this, the term is used in non-technical speech to mean irremediable chaos or disorder. The equation used to calculate physical entropy is very similar to the one used for the texture measure. Its mathematical formula is given below:

$$-\sum_{i,j} P(i,j)\log(P(i,j)$$

However by definition the sum of Pij = 1. With this constraint, the overall maximum of the sum (i.e. of ENT) is 0.5. This maximum is reached when all probabilities are equal. This parameter measures the disorder of an image. When the image is not texturally uniform, many GLCM elements have very small values, which imply that entropy is very large. As an example, consider a window with completely random values of gray level pixel values (white noise). The histogram for such a window is a constant function, all g (i , j) are the same, and the entropy parameter reaches its maximum . From a conceptual point of view, entropy is strongly, but inversely, correlated to GLCM energy. Theoretically, similar results are expected for energy and entropy clustering.

3.5 SUMMARY OF TEXTURE PARAMETERS

Table 3.1 Summary of Textural Parameters

PARAMETER	*DESCRIPTION*	*FORMULA*
CONTRAST	Returns a measure of the intensity contrast between a pixel and its neighbor over the whole image. Range = [0 (size(GLCM) - 1)^2] The Contrast is expected to be low if the gray levels of each pixel pair are similar. Contrast is 0 for a constant image.	$\sum_{i,j} \lvert i-j \rvert^2 P(i,j)$
HOMOGENEITY	Measures the local homogeneity of a pixel pair. The Homogeneity is expected to be large if the gray levels of each pixel pair are similar. Range = [0 1]	$\sum_{i,j} \frac{P(i,j)}{1+\lvert i-j \rvert}$
CORRELATION	Returns a measure of how correlated a pixel is to its neighbor over the whole image. Range = [-1 1] Correlation is 1 or -1 for a perfectly positively or negatively correlated image. The Correlation is expected to be high if the graylevels of the pixel pairs are highly correlated.	$\sum_{i,j} \frac{(i-\mu i)(j-\mu j)P(i,j)}{\sigma_i \sigma_j}$
ENERGY	Measures the number of repeated pairs. The Energy is expected to be high if the occurrence of repeated pixel pairs is high. Energy is 1 for a constant image.	$\sum_{i,j} P(i,j)^2$
ENTROPY	Statistical measure of randomness that can be used to characterize the texture of the input image. The Entropy is expected to be high if the gray levels are distributed randomly through out the image.	$-\sum_{i,j} P(i,j)\log(P(i,j)$

CHAPTER 4

METHODOLOGY USED

MATLAB SOFTWARE

Short for "matrix laboratory", MATLAB is a numerical computing environment and programming language. Created by The MathWorks, MATLAB allows easy matrix manipulation, plotting of functions and data, implementation of algorithms, creation of user interfaces, and interfacing with programs in other languages. MATLAB is built around the MATLAB language, sometimes called M-code or simply M. [http: matlab]

IMAGE PROCESSING TOOLBOX

Image Processing Toolbox is a collection of functions that extend the capability of the MATLAB numeric computing environment. The toolbox supports a wide range of image processing operations. In this work, we have used image processing toolbox of MATLAB version 7.2.

4.3 METHODOLOGY

In this study, an attempt has been made to distinguish normal abdominal CT scan cases from abnormal CT scan cases by studying their textural parameters. Following steps have been performed to achieve this objective.

4.3.1 IMAGE ACQUISITION

The images have been acquired from MRI radiology center, Chandigarh. To avoid any effects on the parameters of images like change in dimensions, change in texture values due to different sources, we have taken all the images from the same source and same CT scan machine. The images taken are that of abdominal CT scan. 20 cases have been taken in which no abnormality is there and 20 cases are taken in which some

abnormality is present. By studying the texture parameters of these images, we have tried to distinguish between the different cases.

4.3.2 IMAGE FORMAT CONVERSION

The images so obtained were in DICOM format. Because the images were in 3D format, the commands of MATLAB could not be used on them. Therefore, to work on the images, they have been converted to BMP format, so that they can easily be used in the MATLAB environment. The syntax used for this purpose is:

I1=rgb2gray(I);

rgb2gray converts RGB images to grayscale by eliminating the hue and saturation information while retaining the luminance. The grayscale image is of 2D type. The images were stored in the workspace of the MATLAB software from where they can be processed.

4.3.3 DETERMINING THE GRAY LEVEL CO OCCURRENCE MATRIX

The gray level co occurrence matrix of the given images is calculated using MATLAB image processing toolbox. The matrix is calculated for every image and in all the 4 directions that is, 0, 45, 90 and 135.

glcm = graycomatrix(I) creates a gray-level co-occurrence matrix (GLCM) from image I.

Graycomatrix creates the GLCM by calculating how often a pixel with gray-level (grayscale intensity) value i occurs horizontally adjacent to a pixel with the value j. Each element (i,j) in glcm specifies the number of times that the pixel with value i occurred horizontally adjacent to a pixel with value j.

Due to the intensive nature of computations involved, only the distances $d = 1$ with angles $\theta = 0°, 45°, 90°$ and 135 °are considered as suggested by Haralick in 1979.

glcm = graycomatrix(I, param1, val1, param2, val2,...) returns one or more gray-level co-occurrence matrices, depending on the values of the optional parameter/value pairs. Parameter names can be abbreviated, and case does not matter. The various parameters are described in the Table 4.1

Table 4.1 GLCM Parameters

PARAMETER	DESCRIPTION
'GRAYLIMITS'	Two-element vector, [low high], that specifies how the grayscale values in I are linearly scaled into gray levels. Grayscale values less than or equal to low are scaled to 1. Grayscale values greater than or equal to high are scaled to NumLevels. If graylimits is set to [], graycomatrix uses the minimum and maximum grayscale values in the image as limits, [min(I(:)) max(I(:))].We have used the minimum and maximum grayscale values as limits.
'OFFSET'	p-by-2 array of integers specifying the distance between the pixel of interest and its neighbor. Each row in the array is a two-element vector, [row offset, column offset], that specifies the relationship, or offset, of a pair of pixels. Row offset is the number of rows between the pixel-of-interest and its neighbor. Column offset is the number of columns between the pixel-of-interest and its neighbor. Because the offset is often expressed as an angle, the following table lists the offset values that specify common angles, given the pixel distance D. Angle Offset 0 [0 D] 45 [-D D] 90 [-D 0] 135 [-D -D] The figure below illustrates the array: offset = [0 1; -1 1; -1 0; -1 -1] 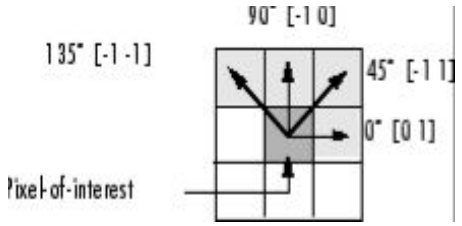 In our study, we have studied the texture parameters in the four directions

	as shown above with a distance between pixel pairs as 1.
'NUMLEVELS'	Integer specifying the number of gray-levels to use when scaling the grayscale values in I. For example, if NumLevels is 8, graycomatrix scales the values in I so they are integers between 1 and 8. The number of gray-levels determines the size of the gray-level co-occurrence matrix (glcm). We have used numlevel value as 8.

SYNTAX used for calculating GLCM of the images was:

glcm = graycomatrix(I,'numlevels', 8, 'G',[],'Offset',[1 0]);

where I is the image whose GLCM is to be calculated

'NUMLEVELS' indicate the number of gray-levels to use when scaling the grayscale values in I. 8 is the number of gray levels we have used that is graycomatrix scales the values in I so they are integers between 1 and 8.

'G' refers to Gray Limits that specifies how the grayscale values in I are linearly scaled into gray levels. We set the gray limits to [], where graycomatrix uses the minimum and maximum grayscale values in the image as limits, [min(I(:)) max(I(:))].

The offset value is used to determine the distance and direction of pixel neighbor. [0 1] is the default value, that is, 0° direction in which the relation between the gray level value of pixel of interest is found out relative to its next right neighbor. We have used four different directions to calculate the values of GLCM, that is, 0°, 45°, 90° and 135°.

4.3.4 DETERMINING CONTRAST, HOMOGENEITY, CORRELATION, ENERGY

After determining the GLCM of images, the texture parameters are found out from the GLCM matrix using the graycoprops command and some programs.

SYNTAX:

var= graycoprops(glcm, properties)

It calculates the statistics specified in properties from the gray level co-occurence matrix.

EXAMPLES:

```
var1 = graycoprops(glcm ,'homogeneity');
var2 = graycoprops(glcm ,'contrast');
var3 = graycoprops(glcm ,'energy');
var3 = graycoprops(glcm ,'correlation');
```

4.3.5 CALCULATION OF ENTROPY

The entropy is not calculated using the above method. Entropy is the measure of randomness of the gray levels in an image, that is, it refers to how much randomly the gray levels are present in an image. The entropy of an image is calculated by first of all finding out the histogram of the images. This histogram is a graph showing the number of pixels in an image at each different intensity value found in that image. From the histogram, the probability of finding a particular gray level value in whole image is found out. It is done by dividing the gray level value by the sum of all gray level values in the image. From the probabilities, we find out the entropy function of the image by applying the entropy formula.

$$-\sum_{i,j} P(i,j)\log(P(i,j)$$

Where P_{ij} represents the number of occurrences of grey levels i and j within the given window, given a certain (δ, θ) pair;

CHAPTER 5

RESULTS AND DISCUSSIONS

5.1 INTRODUCTION

The various texture parameters have been found of different CT scan images of abdomen. 20 normal abdomen CT scan images have been taken and their textural parameters - contrast, homogeneity, correlation, energy, and entropy have been calculated. Similarly, same textural parameters of abnormal CT scan images have also been calculated and compared with normal values.

Some examples of normal CT scan images of abdomen are shown in Figure 5.1(a) to 5.1(d). These images are of subjects with no proven clinical abnormality.

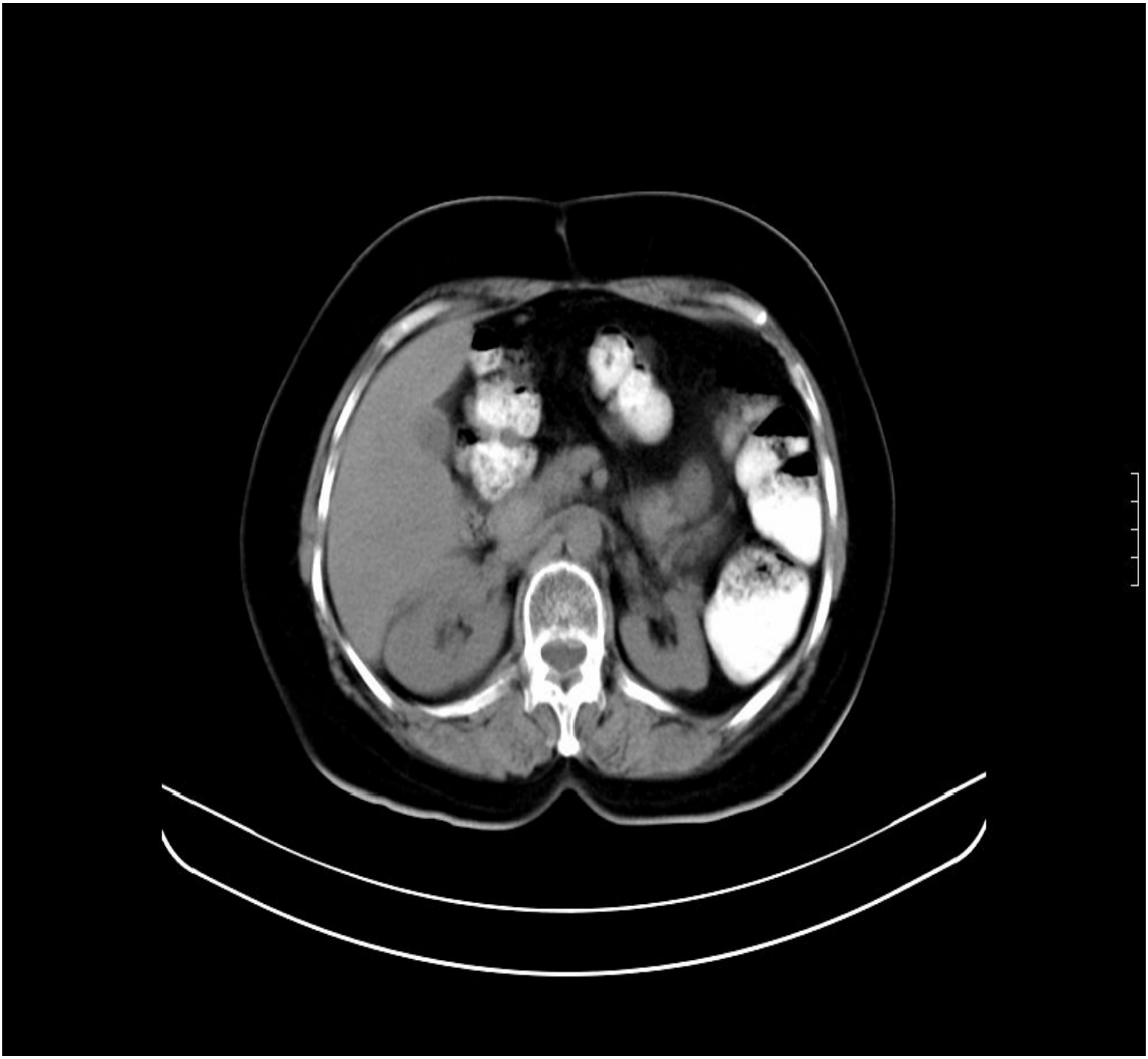

Figure 5.1(a) Normal Image 001

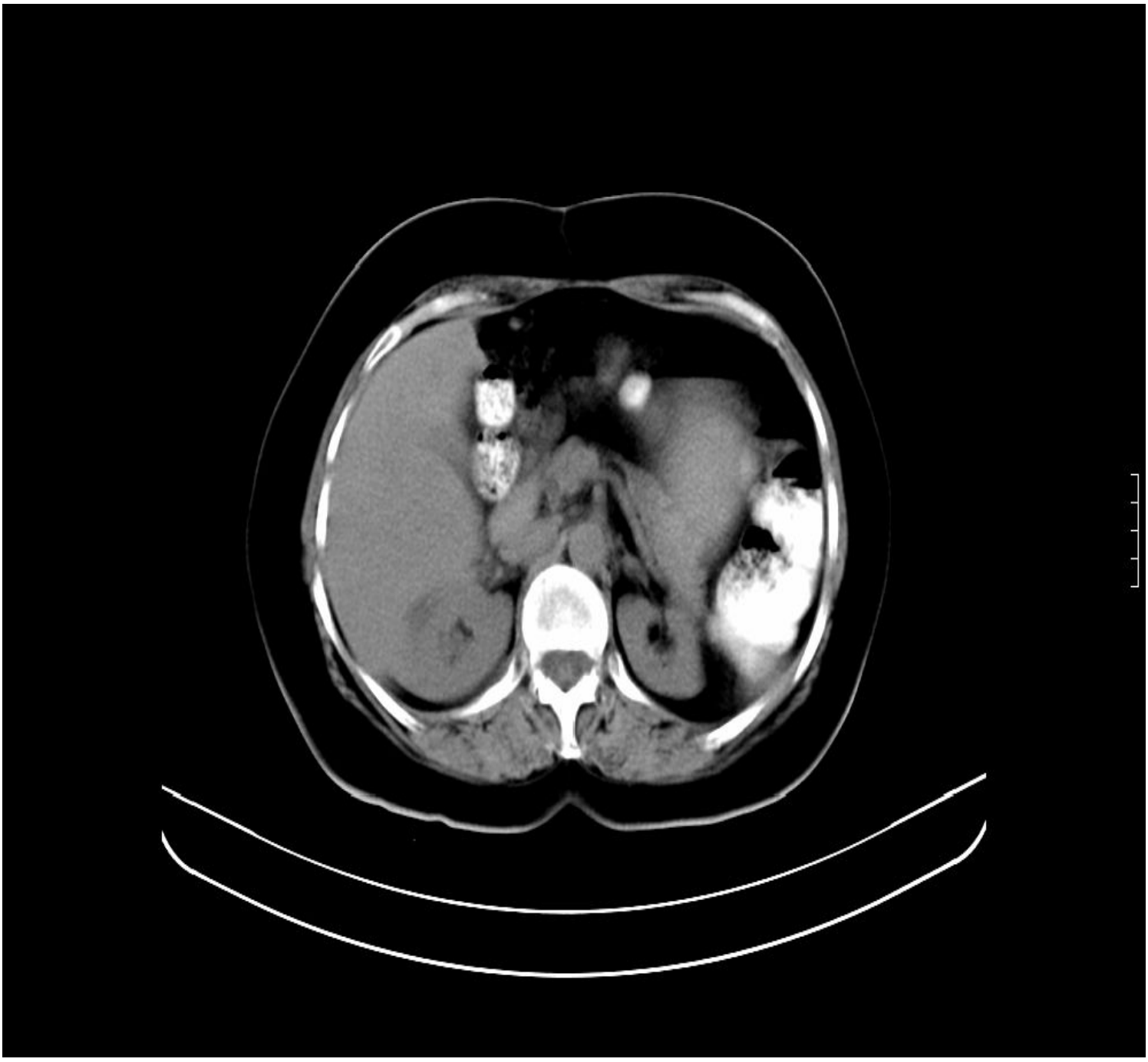

Figure 5.1(b) Normal Image 002

Figure 5.1 (c) Normal Image 003

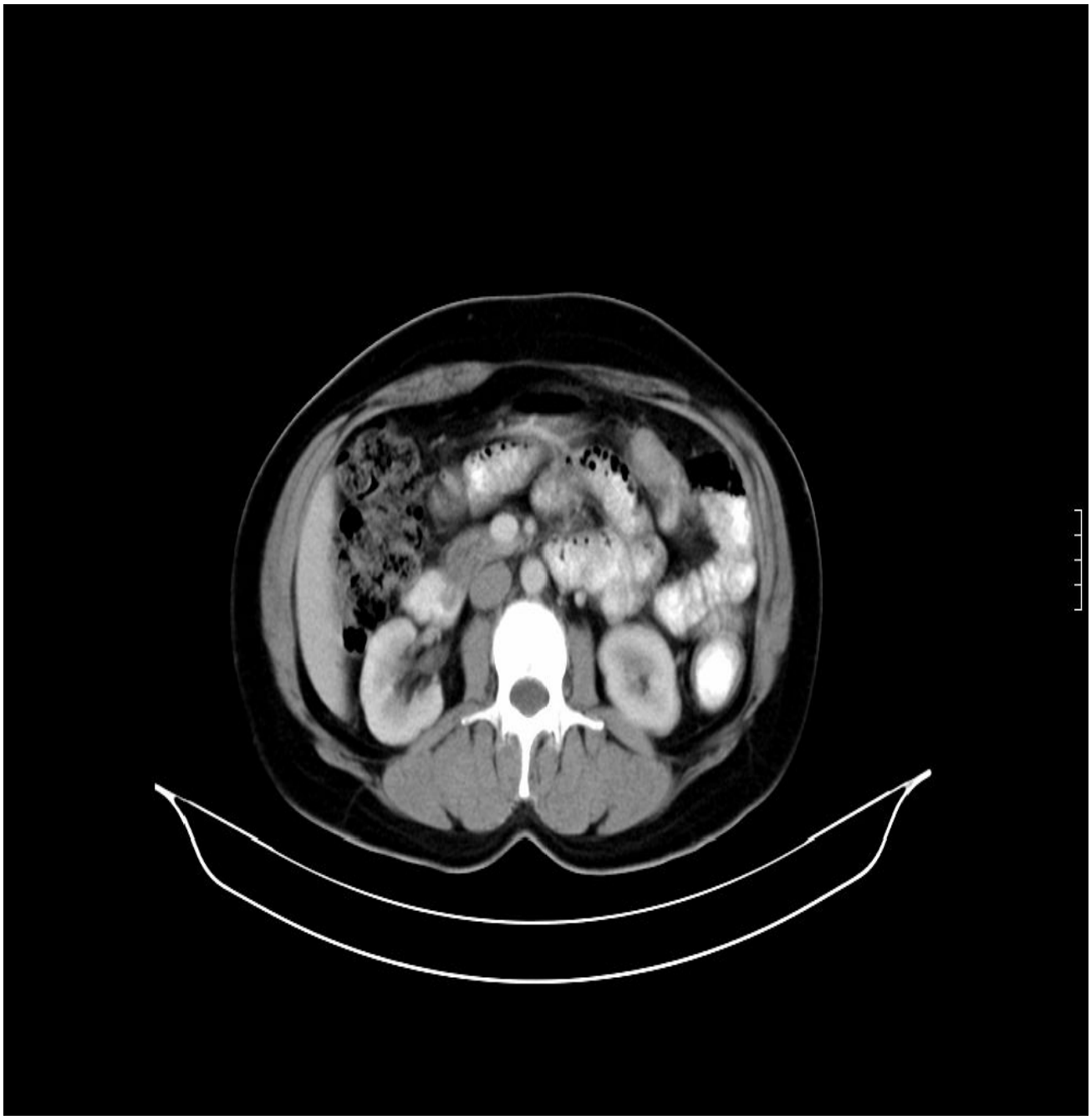

Figure 5.1 (d) Normal Images

Some examples of abnormal CT scan images of abdomen are shown in Figure 5.2(a) to 5.2(d). These images are of subjects with proven clinical abnormality.

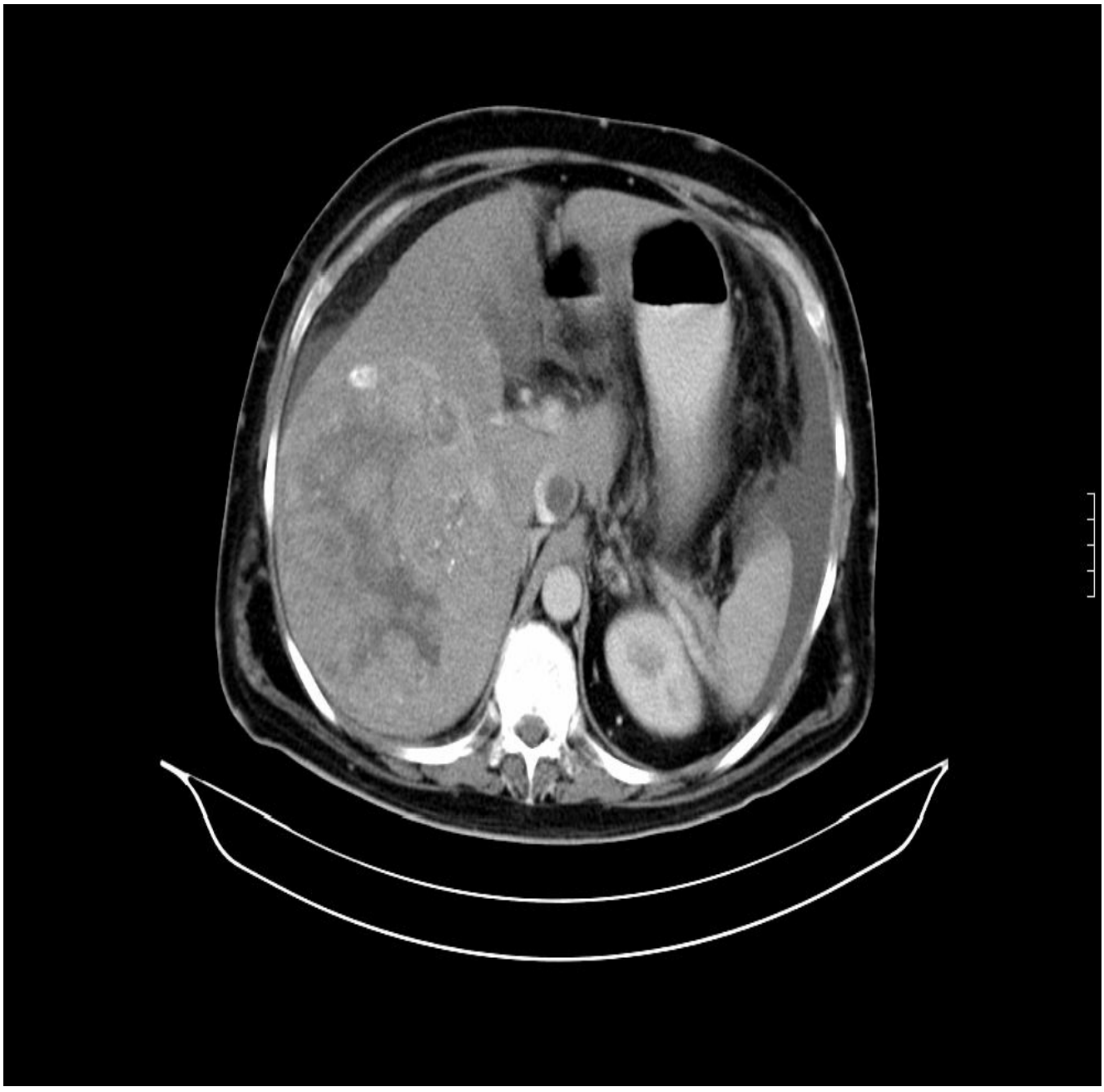

Figure 5.2 (a) Abnormal Image 001

Figure 5.2 (b) Abnormal Image 002

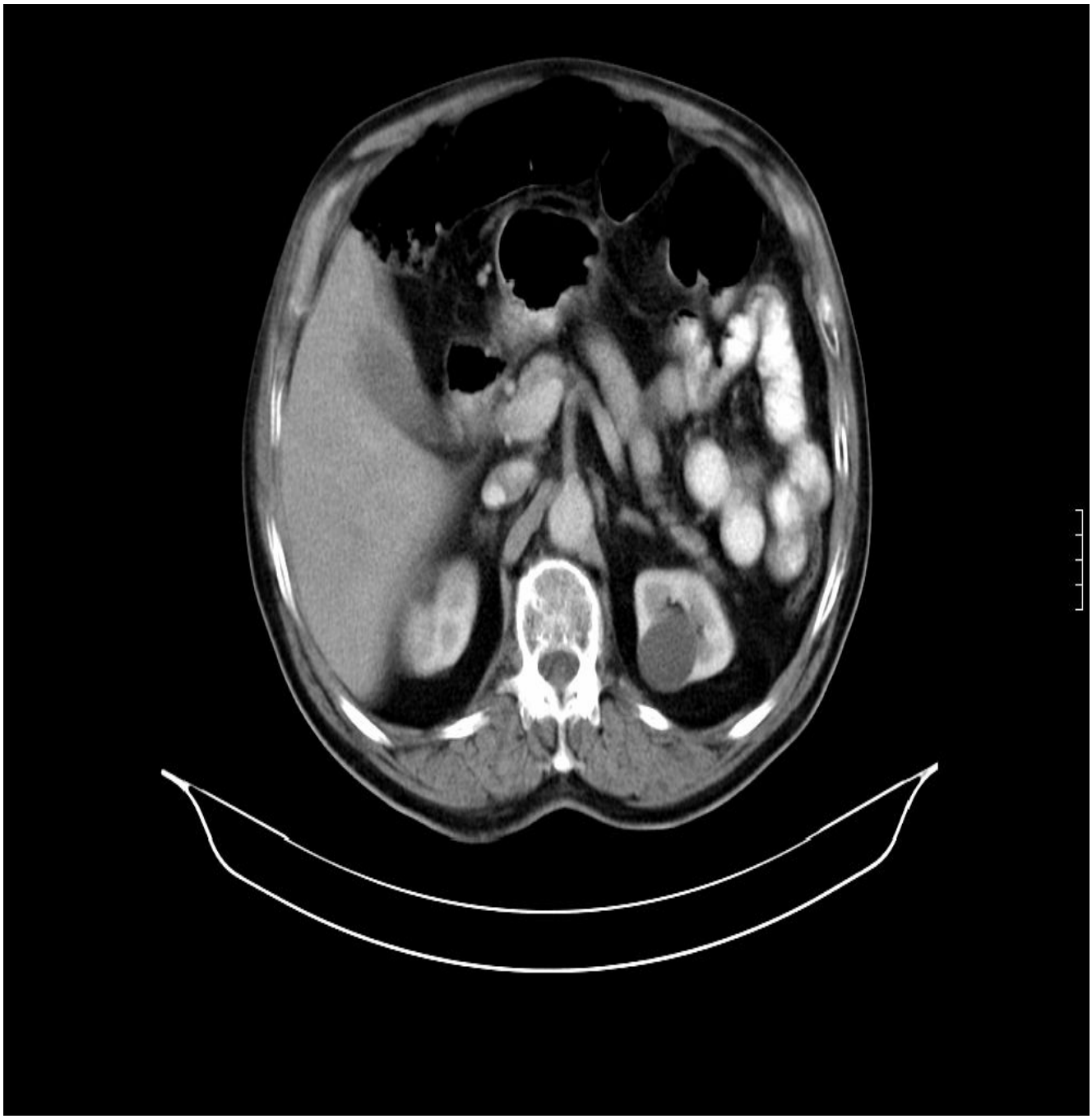

Figure 5.2 (c) Abnormal Image 003

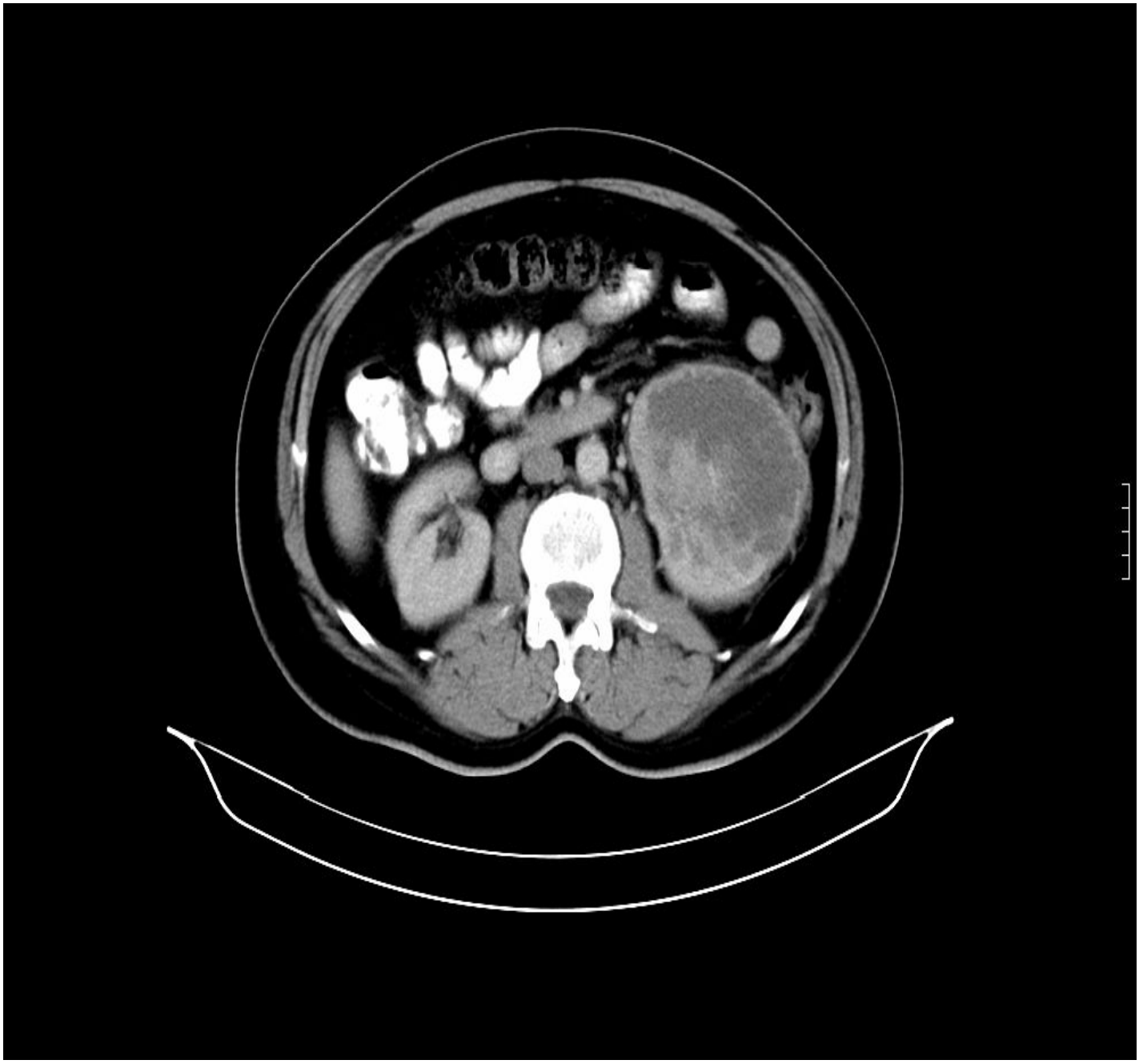

Figure 5.2 (d) Abnormal Image 004

5.2 RESULTS

We have coded CT scan images taken for this study as IMG001 to IMG020 for normal cases and IMG101 to IMG120 for abnormal cases. Contrast values calculated for all these cases have been tabulated in tables 5.1 & 5.2. Homogeneity for normal and abnormal cases have been tabulated in tables 5.3 & 5.4. Correlation values are in table 5.5 & 5.6 and energy parameter values are in tables 5.7 & 5.8. Entropy parameter is tabulated in 5.9 & 5.10.

5.2.1 CONTRAST VALUES FOR NORMAL AND ABNORMAL CASES

Table 5.1 Contrast values for normal cases

ANGLE→ IMAGE NO.	0º	45º	90º	135º
001	0.0821	0.2552	0.2177	0.1963
002	0.0780	0.2394	0.2035	0.2606
003	0.0844	0.2416	0.1985	0.2452
004	0.1022	0.2688	0.2236	0.2400
005	0.0702	0.2854	0.2241	0.2830
006	0.0708	0.2140	0.1811	0.2773
007	0.0863	0.2487	0.2057	0.2111
008	0.0759	0.2284	0.1969	0.2495
009	0.0679	0.2122	0.1856	0.2334
010	0.0690	0.2268	0.1960	0.2197
011	0.0922	0.2597	0.2136	0.2396
012	0.0840	0.2422	0.2034	0.2608
013	0.0837	0.2568	0.2686	0.2439
014	0.0776	0.2411	0.2167	0.2592
015	0.0920	0.2601	0.2052	0.2208
016	0.0921	0.2673	0.2250	0.2379
017	0.0763	0.2204	0.1853	0.2284
018	0.0774	0.2322	0.2670	0.2340
019	0.0763	0.2290	0.1999	0.2345
020	0.0764	0.2264	0.1955	0.2234
MEAN	***0.0807***	***0.2427***	***0.2106***	***0.2399***
MAX.	***0.1022***	***0.2854***	***0.2686***	***0.2830***
MIN.	***0.0679***	***0.2122***	***0.1811***	***0.1963***

Table 5.2 Contrast values for abnormal cases

ANGLE→ IMAGE NO.	**0º**	**45º**	**90º**	**135º**
101	0.1501	0.3679	0.2882	0.3538
102	0.1438	0.3617	0.2855	0.3534
103	0.1077	0.2756	0.2274	0.2805
104	0.1011	0.2291	0.1937	0.2201
105	0.1040	0.2708	0.2254	0.2643
106	0.1369	0.2631	0.2209	0.2698
107	0.1006	0.3615	0.2163	0.2624
108	0.1098	0.2700	0.2915	0.3492
109	0.1027	0.2625	0.2224	0.2015
110	0.1129	0.2680	0.2194	0.5049
111	0.1072	0.2708	0.2245	0.4782
112	0.1068	0.2231	0.2227	0.2689
113	0.1170	0.2679	0.1938	0.2764
114	0.1098	0.2654	0.2254	0.2744
115	0.1145	0.2771	0.2016	0.2242
116	0.1235	0.2381	0.2143	0.2713
117	0.1008	0.2688	0.2136	0.2609
118	0.1065	0.2639	0.2097	0.2408
119	0.1245	0.2612	0.2343	0.2695
120	0.1012	0.2768	0.2443	0.2653
MEAN	***0.1138***	***0.2768***	***0.2287***	***0.2944***
MAX.	***0.1501***	***0.3679***	***0.2915***	***0.5049***
MIN.	***0.1006***	***0.2231***	***0.1937***	***0.2015***

5.2.1.1 CONTRAST COMPARISON:

1) For 0º direction

The mean value for normal cases is 0.0807. The maximum and minimum values are 0.1022 and 0.0679. It has been concluded that all the values lies between 0.0807 ± 38% range for normal cases.

For abnormal cases, the mean value is 0.1138. The maximum and minimum value are 0.1501 and 0.1006. The ranges of values for abnormal cases are thus found out to be 0.1138 ± 44%.

Therefore, from the above data it can be seen that out of 20 cases, in 19 cases we have been able to get different ranges of contrast in normal cases and abnormal cases. Hence, we can say that for 0º direction, we get 95% accurate results for distinguishing between normal and abnormal cases.

2) For 45º direction

For normal cases, the mean value is found out to be 0.2427. The maximum and minimum values are 0.2854 and 0.2122. It has been concluded that all the values lies between range 0.2427 ± 18.5%.

For abnormal cases, the mean value is 0.2768 and the maximum & minimum values are 0.3679 & 0.2231 respectively. All the values lie in the range 0.2768 ± 34.3%.

Since the range of values is not different in normal and abnormal cases, therefore no definite results can be arrived at from this data.

3) For 90º direction

The mean value for normal cases is 0.2106.themaximum and minimum values are 0.2686 and 0.1811. It has been concluded that all the values lies between ranges 0.2106 ± 21.8% for normal cases.

For abnormal cases, the mean value is 0.2287. The maximum and minimum value are 0.2915 and 0.1937. The ranges of values for abnormal cases are thus found out to be 0.2287 ± 28.4%.

Due to same range of contrast in normal and abnormal cases for 90º angle, we were not able to distinguish between different cases.

4) For 135º direction

For normal cases, the mean value is found out to be 0.2399. The maximum and minimum values are 0.2830 and 0.1963. It has been concluded that all the values lies between range 0.2399 ± 20.8%.

For abnormal cases, the mean value is 0.2944 and the maximum & minimum values are 0.5049 & 0.2015 respectively. All the values lie in the range 0.2944 ± 71%.

Since the range of values is not different in normal and abnormal cases for contrast, therefore no definite results can be arrived at from this data.

5.2.2 HOMOGENEITY VALUES FOR NORMAL AND ABNORMAL CASES

Table 5.3 Homogeneity values for normal cases

ANGLE→ IMAGE NO.	**0º**	**45º**	**90º**	**135º**
001	0.9787	0.9680	0.9737	0.9680
002	0.9772	0.9659	0.9726	0.9655
003	0.9764	0.9651	0.9723	0.9656
004	0.9702	0.9559	0.9648	0.9550
005	0.9622	0.9472	0.9605	0.9481
006	0.9801	0.9699	0.9761	0.9681
007	0.9786	0.9680	0.9742	0.9683
008	0.9791	0.9683	0.9747	0.9736
009	0.9832	0.9742	0.9779	0.9669
010	0.9792	0.9668	0.9734	0.9608
011	0.9743	0.9618	0.9734	0.9670
012	0.9784	0.9663	0.9684	0.9529
013	0.9684	0.9536	0.9728	0.9673
014	0.9771	0.9672	0.9623	0.9587
015	0.9725	0.9602	0.9732	0.9698
016	0.9793	0.9691	0.9721	0.9461
017	0.9792	0.9695	0.9680	0.9863
018	0.9625	0.9474	0.9744	0.9655
019	0.9790	0.9768	0.9761	0.9669
020	0.9787	0.9680	0.9567	0.9667
MEAN	***0.9757***	***0.9644***	***0.9708***	***0.9643***
MAX.	***0.9832***	***0.9768***	***0.9779***	***0.9863***
MIN.	***0.9622***	***0.9472***	***0.9567***	***0.9461***

Table 5.4 Homogeneity values for abnormal cases

ANGLE→ IMAGE NO.	0º	45º	90º	135º
101	0.9791	0.9697	0.9743	0.9689
102	0.9778	0.9682	0.9733	0.9760
103	0.9666	0.9513	0.9618	0.9512
104	0.9817	0.9703	0.9749	0.9711
105	0.9656	0.9501	0.9646	0.9504
106	0.9701	0.9567	0.9666	0.9563
107	0.9666	0.9520	0.9715	0.9511
108	0.9716	0.9584	0.9711	0.9577
109	0.9768	0.9656	0.9743	0.9652
110	0.9759	0.9647	0.9710	0.9751
111	0.9771	0.9677	0.9718	0.9680
112	0.9751	0.9640	0.9727	0.9635
113	0.9785	0.9663	0.9656	0.9648
114	0.9649	0.9505	0.9597	0.9508
115	0.9693	0.9566	0.9756	0.9564
116	0.9656	0.9501	0.9637	0.9504
117	0.9803	0.9704	0.9643	0.9703
118	0.9638	0.9506	0.9655	0.9514
119	0.9657	0.9522	0.9701	0.9544
120	0.9666	0.9357	0.9654	0.9514
MEAN	***0.9719***	***0.9585***	***0.9688***	***0.9602***
MAX.	***0.9817***	***0.9704***	***0.9756***	***0.9760***
MIN.	***0.9638***	***0.9357***	***0.9597***	***0.9504***

5.2.2.1 HOMOGENEITY COMPARISON:

1) For 0^o direction

The mean value for normal cases is 0.9757. The maximum and minimum values are 0.9832 and 0.9622. It has been concluded that all the values lies between 0.9757 ± 1.4% range for normal cases.

For abnormal cases, the mean value is 0.9719. The maximum and minimum value are 0.9817 and 0.9638. The ranges of values for abnormal cases are thus found out to be 0.9719 ± 1%.

From the above tables, we can see that there is no difference between homogeneity values of normal and abnormal cases for this direction.

2) For 45^o direction

For normal cases, the mean value is found out to be 0.9644. The maximum and minimum values are 0.9768 and 0.9472. It has been concluded that all the values lies between range 0.9644 ± 2%.

For abnormal cases, the mean value is 0.9585 and the maximum & minimum values are 0.9704 & 0.9357 respectively. All the values lie in the range 0.9585 ± 2.5%.

The range of homogeneity for normal and abnormal cases is same for this direction. Hence, we cannot distinguish between different cases for this data.

3) For 90^o direction

The mean value for normal cases is 0.2106.themaximum and minimum values are 0.2686 and 0.1811. It has been concluded that all the values lies between ranges 0.2106 ± 21.8% for normal cases.

For abnormal cases, the mean value is 0.2287. The maximum and minimum values are 0.2915 and 0.1937. The ranges of values for abnormal cases are thus found out to be 0.2287 ± 28.4%.

From the above tables, it can be seen that there is no difference between homogeneity values of normal and abnormal cases for this direction.

4) For 135^{o} direction

For normal cases, the mean value is found out to be 0.9643. The maximum and minimum values are 0.9863 and 0.9461. It has been concluded that all the values lies between range 0.9643 ± 2.2%.

For abnormal cases, the mean value is 0.9602 and the maximum & minimum values are 0.9760 & 0.9504 respectively. All the values lie in the range 0.9602 ± 1.6%.

The range of homogeneity values is not different for normal cases and abnormal cases. Hence, this data is not sufficient for distinguishing normal and abnormal cases.

5.2.3 CORRELATION VALUES FOR NORMAL AND ABNORMAL CASES

Table 5.5 Correlation values for normal cases

ANGLE→ IMAGE NO.	**0º**	**45º**	**90º**	**135º**
001	0.9836	0.9491	0.9565	0.9480
002	0.9841	0.9513	0.9586	0.9502
003	0.9833	0.9523	0.9608	0.9526
004	0.9826	0.9543	0.9620	0.9519
005	0.9792	0.9273	0.9603	0.9508
006	0.9759	0.9367	0.9476	0.9283
007	0.9780	0.9541	0.9604	0.9365
008	0.9847	0.9563	0.9618	0.9531
009	0.9860	0.9671	0.9715	0.9548
010	0.9900	0.9549	0.9629	0.9652
011	0.9840	0.9647	0.9703	0.9547
012	0.9877	0.9611	0.9552	0.9644
013	0.9848	0.9469	0.9583	0.9604
014	0.9827	0.9510	0.9706	0.9501
015	0.9842	0.9650	0.9610	0.9626
016	0.9869	0.9534	0.9656	0.9648
017	0.9879	0.9562	0.9624	0.9533
018	0.9838	0.9563	0.9664	0.9543
019	0.9814	0.9607	0.9559	0.9553
020	0.9854	0.9492	0.9545	0.9608
MEAN	***0.9838***	***0.9533***	***0.9611***	***0.9536***
MAX.	***0.9900***	***0.9671***	***0.9715***	***0.9652***
MIN	***0.9759***	***0.9273***	***0.9476***	***0.9283***

Table 5.6 Correlation values for abnormal cases

ANGLE→ IMAGE NO.	**0º**	**45º**	**90º**	**135º**
101	0.9740	0.9362	0.9500	0.9387
102	0.9775	0.9435	0.9554	0.9448
103	0.9825	0.9552	0.9630	0.9544
104	0.9898	0.9649	0.9703	0.9663
105	0.9794	0.9436	0.9541	0.9469
106	0.9844	0.9557	0.9630	0.9575
107	0.9817	0.9524	0.9611	0.9672
108	0.9881	0.9671	0.9730	0.9373
109	0.9813	0.9507	0.9602	0.9282
110	0.9772	0.9361	0.9474	0.9387
111	0.9742	0.9292	0.9414	0.9645
112	0.9779	0.9403	0.9499	0.9452
113	0.9775	0.9395	0.9502	0.9592
114	0.9894	0.9646	0.9693	0.9469
115	0.9778	0.9459	0.9555	0.9381
116	0.9842	0.9599	0.9662	0.9449
117	0.9794	0.9436	0.9541	0.9496
118	0.9797	0.9388	0.9481	0.9510
119	0.9769	0.9450	0.9561	0.9289
120	0.9800	0.9499	0.9594	0.9345
MEAN	***0.9806***	***0.9481***	***0.9573***	***0.9471***
MAX.	***0.9898***	***0.9671***	***0.9730***	***0.9672***
MIN.	***0.9740***	***0.9292***	***0.9414***	***0.9282***

5.2.3.1 CORRELATION COMPARISON

1) For 0^o direction

The mean value for normal cases is 0.9838. The maximum and minimum values are 0.9900 and 0.9759. It has been concluded that all the values lies between 0.9838 ± 1% range for normal cases.

For abnormal cases, the mean value is 0.9806. The maximum and minimum value are 0.9898 and 0.9740. The ranges of values for abnormal cases are thus found out to be 0.9806 ± 1%.

The values of correlation for normal and abnormal cases for this direction are not found to be different. Hence, further study is required.

2) For 45^o direction

For normal cases, the mean value is found out to be 0.9533.The maximum and minimum values are 0.9671 and 0.9273. It has been concluded that all the values lies between range 0.9533 ± 3.1%.

For abnormal cases, the mean value is 0.9481 and the maximum & minimum values are 0.9671 & 0.9292 respectively. All the values lie in the range 0.9481± 2.1%.

Correlation values are same for normal and abnormal cases for this direction. Therefore this parameter is not sufficient to differentiate between normal and abnormal cases.

3) For 90^o direction

The mean value for normal cases is 0.9611.themaximum and minimum values are 0.9715 and 0.9476. It has been concluded that all the values lies between ranges 0.9611 ± 2% for normal cases.

For abnormal cases, the mean value is 0.9573. The maximum and minimum value are 0.9730 and 0.9414. The ranges of values for abnormal cases are thus found out to be 0.9573 ± 1.6%.

The values of correlation for normal and abnormal cases for this direction are not found to be different. Hence, further study is required.

4) For 135^{o} direction

For normal cases, the mean value is found out to be 0.9536. The maximum and minimum values are 0.9652 and 0.9283. It has been concluded that all the values lies between range 0.9536 ±3.1%.

For abnormal cases, the mean value is 0.9471 and the maximum & minimum values are 0.9672 & 0.9282 respectively. All the values lie in the range 0.9471 ± 2.1%.

Since the range of values is not different in normal and abnormal cases for homogeneity, therefore no definite results can be arrived at from this data.

5.2.4 ENERGY VALUES FOR NORMAL AND ABNORMAL CASES

Table 5.7 Energy values for normal cases

ANGLE→ IMAGE NO.	**0º**	**45º**	**90º**	**135º**
001	0.6677	0.6610	0.6638	0.6611
002	0.6560	0.6492	0.6523	0.6492
003	0.6980	0.6915	0.6947	0.6918
004	0.5931	0.5850	0.5895	0.5846
005	0.5365	0.5277	0.5340	0.5385
006	0.7327	0.7251	0.7287	0.7255
007	0.7323	0.7256	0.7290	0.7258
008	0.6730	0.6665	0.6692	0.6665
009	0.7379	0.7314	0.7336	0.7308
010	0.5947	0.5880	0.5907	0.5879
011	0.6439	0.6367	0.6399	0.6366
012	0.6582	0.6520	0.6545	0.6522
013	0.6075	0.5997	0.6037	0.5995
014	0.6587	0.6521	0.6547	0.6521
015	0.6596	0.5640	0.6559	0.6529
016	0.5708	0.6503	0.5673	0.5631
017	0.6560	0.6580	0.6530	0.6504
018	0.6642	0.5796	0.6612	0.6580
019	0.6706	0.6641	0.6607	0.5788
020	0.6652	0.6580	0.6779	0.6640
MEAN	***0.6538***	***0.6432***	***0.6507***	***0.6434***
MAX.	***0.7379***	***0.7314***	***0.7336***	***0.7308***
MIN.	***0.5365***	***0.5277***	***0.5340***	***0.5385***

Table 5.8 Energy values for abnormal cases

ANGLE→ IMAGE NO.	**0º**	**45º**	**90º**	**135º**
101	0.7489	0.7425	0.7459	0.7427
102	0.7224	0.7159	0.7193	0.7161
103	0.4969	0.4887	0.4936	0.4890
104	0.6214	0.6143	0.6167	0.6146
105	0.5342	0.5188	0.5289	0.5200
106	0.4723	0.4619	0.4684	0.4616
107	0.4571	0.4503	0.4539	0.4499
108	0.4817	0.4755	0.4783	0.4753
109	0.6952	0.6883	0.6917	0.7019
110	0.7089	0.7020	0.7056	0.7503
111	0.7572	0.7501	0.7541	0.6971
112	0.7046	0.6976	0.7012	0.7088
113	0.7158	0.7087	0.5219	0.5024
114	0.5267	0.5190	0.7126	0.7407
115	0.5100	0.5022	0.5070	0.5476
116	0.5324	0.5261	0.5298	0.5307
117	0.5342	0.5188	0.5288	0.5352
118	0.7473	0.7409	0.5533	0.5200
119	0.5551	0.5471	0.5357	0.4563
120	0.5383	0.5304	0.5405	0.4322
MEAN	***0.6030***	***0.5949***	***0.5893***	***0.5796***
MAX.	***0.7572***	***0.7501***	***0.7541***	***0.7503***
MIN.	***0.4571***	***0.4503***	***0.4539***	***0.4322***

5.2.4.1 ENERGY COMPARISON

1) For 0^{o} direction

The mean value for normal cases is 0.6538. The maximum and minimum values are 0.7379 and 0.5365. It has been concluded that all the values lies between 0.6538 ± 18.35% ranges for normal cases.

For abnormal cases, the mean value is 0.6030. The maximum and minimum values are 0.7572 and 0.4571. The ranges of values for abnormal cases are thus found out to be 0.6030 ± 24.8%.

For energy parameter, it has been found out that for 60% of the cases, different range is there for normal and abnormal cases. The range for normal cases is from 0.7379 to 0.5365. 12 cases out of 20 for abnormal cases lie out of this range, that is, above 0.7379 and below 0.5365.

2) For 45^{o} direction

For normal cases, the mean value is found out to be 0.6432.The maximum and minimum values are 0.7314 and 0.5277. It has been concluded that all the values lies between range 0.6432 ± 18.6%.

For abnormal cases, the mean value is 0.5949 and the maximum & minimum values are 0.7501 & 0.4503 respectively. All the values lay in the range 0.5949± 26.8%.for both normal and abnormal cases.

For this direction, 11 cases have been found out to have different range. Further study is required for this parameter.

3) For 90^{o} direction

The mean value for normal cases is 0.6507.themaximum and minimum values are 0.7336 and 0.5340. It has been concluded that all the values lies between ranges 0.6507 ±18.4% for normal cases.

For abnormal cases, the mean value is 0.5893. The maximum and minimum values are 0.7541 and 0.4539. The ranges of values for abnormal cases are thus found out to be 0.5893 ± 33.9%.

Since the range of values is not different in normal and abnormal cases for energy, therefore no definite results can be arrived at from this data.

4) For 135^{o} direction

For normal cases, the mean value is found out to be 0.6434. The maximum and minimum values are 0.7308 and 0.5385. It has been concluded that all the values lies between range 0.6434 ± 18.6 %.

For abnormal cases, the mean value is 0.5796 and the maximum & minimum values are 0.7503 & 0.4322 respectively. All the values lie in the range 0.5796 ±31%.

70% of abnormal cases are found to have different range of this parameter from normal cases.

5.2.5 ENTROPY VALUES FOR NORMAL AND ABNORMAL CASES

Table 5.9 Entropy values for normal cases

IMAGE NO.	ENTROPY
001	2.0528
002	2.3169
003	2.1047
004	2.8267
005	2.2830
006	2.1560
007	2.6875
008	2.5096
009	2.2439
010	2.4026
011	2.0688
012	2.6950
013	2.0821
014	2.3453
015	2.5843
016	2.2972
017	2.4087
018	2.4152
019	2.4217
020	2.4281
MEAN	***2.4346***
MAX.	***2.8267***
MIN.	***2.0528***

Table 5.10 Entropy values for abnormal cases

IMAGE NO.	ENTROPY
101	1.3841
102	1.5125
103	3.3790
104	3.1866
105	3.3730
106	3.4974
107	3.2570
108	1.6298
109	1.8705
110	1.5526
111	1.8505
112	1.7780
113	3.0331
114	3.1700
115	3.0429
116	3.1877
117	1.6737
118	3.0422
119	3.1301
120	3.0806
MEAN	***2.5815***
MAX.	***3.4974***
MIN.	***1.3841***

5.2.5.1 ENTROPY COMPARISON

The mean value of entropy parameter for normal cases is found out to be 2.4346. The maximum value is 2.8267 and minimum is 2.0528. The range of the values is 2.4346 ± 16.4%.

For abnormal cases, the mean value is 2.5815. The maximum and minimum values are 3.4974 and 1.3841. The range of values is 2.5815 ± 46.4%.

For entropy, it can be clearly seen from the tables that the range of normal cases is entirely different from that of abnormal cases. The normal cases range is found to be from 2.8267 to 2.0528. All the values for abnormal cases either lie above the maximum value of normal images, that is, 2.8267 or below its minimum value, that is, 2.0528. Hence, this parameter shows 100% results for distinguishing between abnormal images from normal images.

The table has been arranged in ascending order of the entropy values in table 5.11. It clearly shows the range difference between the normal values and the abnormal values. The underlined values show the abrupt change in values of range for abnormal entropy values.

Table 5.11 Entropy values in ascending order

IMAGE NO.	ENTROPY
101	1.3841
102	1.5125
110	1.5526
108	1.6298
117	1.6737
112	1.7780
111	1.8505
109	1.8705
113	3.0331
118	3.0422
115	3.0429
120	3.0806
119	3.1301
114	3.1700
104	3.1866
116	3.1877
107	3.2570
105	3.3730
103	3.3790
106	3.4974

5.4 CONCLUSION

From the results above, it has been concluded that out of five textural parameters- contrast, homogeneity, correlation, energy, and entropy, some of the parameters have given good results. For entropy, it can be concluded that it has been able to distinguish between normal cases of CT scan from abnormal cases with 100% accuracy. For all the 20 cases taken, it has given different values for normal images and abnormal images. The normal cases range is found to be from 2.8267 to 2.0528. All the values for abnormal cases either lie above the maximum value of normal images, that is, 2.8267 or below its minimum value, that is, 2.0528. Hence, this parameter shows 100% results for distinguishing between abnormal images from normal images.

It is seen from the data that out of 20 cases, in 19 cases we have been able to get different ranges of contrast in normal cases and abnormal cases. For contrast, 95% accurate results are there for the 0º direction.

For the rest of the parameters, no definite results are found out. Hence, further study is suggested.

5.5 FUTURE SCOPE

The study presented here is small part of the texture analysis of medical images. Here, a small number of images are taken which are not sufficient to statistically prove the results of this thesis work. In order to arrive to definite conclusions, it is necessary to study a larger number of images.

All the images taken in this study are from the same CT scan machine. To take this study step further, images from different CT scan machines can be taken to study the effects of taking data from different sources.

Only CT scan images of abdomen are studied in this work. Images of other body parts can be taken to see if the same results also apply to them or not. In addition, other images like MRI, Ultrasound, X ray images etc. can also be taken and effects of various parameters can be studied on them.

REFERENCES

[Chung-Ming et. al., 1992] Chung-Ming W.;Yung-Chang Chen; Kai-Sheng Hsieh; "Texture features for classification of ultrasonic liver images" Medical Imaging, IEEE Transactions on Vol No. 11, Issue 2, 1992, Page(s): 141 - 152

[Clausi et. al., 2002] Clausi, David A.; Can. J.; "An analysis of co-occurrence texture statistics as a function of grey level quantization", Remote Sensing, Vol. No. 28, Issue 1, 2002, Page(s): 45 - 62

[DaPonte et. al., 1988] DaPonte, J.S.; Gelber, J.; Fox, M.D.; "Effect of cooccurrence displacement vector on quantization of ultrasonic image texture" Bioengineering Conference, Proceedings of the 1988 Fourteenth Annual Northeast, 1988, Page(s): 298 - 300

[Felipe et. al., 2003] Felipe, J.C.; Traina, A.J.M.; Traina, C., Jr.; "Retrieval by content of medical images using texture for tissue identification", Computer-Based Medical Systems, 2003. Proceedings 16th IEEE Symposium 26-27, 2003, Page(s): 175 - 180

[Haralick et. al., 1973] Haralick, Robert M.; Shanmugam, K.; Dinstein ; "Textural Features for Image Classification", IEEE Transactions on Systems, Man and Cybernetics, Vol. No. 3, Issue 6, 1973, Page(s): 610 - 621

[Haralick, 1979] R. Haralick; "Statistical and Structural Approaches to Texture", Proceedings IEEE 67, 1979, Page(s): 786 - 804

[Ji et. al., 2000] Ji, Q.; Engel, J.; Craine, E.; "Texture analysis for classification of cervix lesions", Medical Imaging, IEEE Transactions on Vol. No. 19, Issue 11, 2000, Page(s): 1144 - 1149

[Kovalev et. al., 2001] Kovalev, V.A.; Kruggel, F.; Gertz, H.-J.; von Cramon, D.Y.; "Three-dimensional texture analysis of MRI brain datasets", Medical Imaging, IEEE Transactions on Vol. No. 20, Issue 5, 2001, Page(s): 424 - 433

[Kyriacou et. al., 1998] Kyriacou, E.; Pavlopoulos, S.; Konnis, G.; Koutsouris, D.; Zoumpoulis, P.; Theotokas, L.; "Computer assisted characterization of diffused liver disease using image texture analysis techniques on B-scan images", Nuclear Science Symposium, 1997. IEEE Vol. 2, 1998, Page(s): 1479 - 1483

[Mir et. al., 1995] A. H. Mir, M. Hanmandlu, S. N. Tandon, "Texture analysis of CT images", IEEE Eng. Medical Biology Magazine, Vol. No. 14, 1995, Page(s): 781 - 786

[Pavlopoulos et. al., 1996] Pavlopoulos, S.; Konnis, G.; Kyriacou, E.; Koutsouris, D.; Zoumpoulis, P.; Theotokas, I.; "Evaluation of texture analysis techniques for quantitative characterization of ultrasonic liver images", Engineering in Medicine and Biology Society, Bridging Disciplines for Biomedicine. Proceedings of the 18th Annual International Conference of the IEEE Vol. No. 3, 1996, Page(s): 1151 - 1152

[Sharma and Singh, 2001] Sharma, M.; Singh, S.; "Evaluation of texture methods for image analysis", Intelligent Information Systems Conference, The Seventh Australian and New Zealand, 2001, Page(s): 117 - 121

[Sheppard and Liwen, 2007] Sheppard, M.A.; Liwen Shih; "P6C-2 Image Texture Clustering for Prostate Ultrasound Diagnosis", Ultrasonics Symposium, 2007. IEEE 28-31, 2007, Page(s): 2473 - 2476

[Sun et. al., 1996] Sun Y.N.; Horng, M.-H.; Lin, X.Z.; Wang, J.-Y.; "Ultrasonic image analysis for liver diagnosis", Engineering in Medicine and Biology Magazine, IEEE Vol. No. 15, Issue 6, 1996, Page(s): 93 - 101

[Wang et. al., 2002] Wang Y.; Itoh K.; Taniguchi N.; Toei H.; Kawai F.; Nakamura M.; Omoto K.; Yokota K.; Ono T.; "Studies on tissue characterization by texture analysis with co-occurrence matrix method using ultra sonography and CT imaging", Journal of Medical Ultrasonics; Vol. No. 29, Issue 4, 2002, Page(s): 211 - 223

BIBLIOGRAPHY

1) Rafael C Gonzalez, Richard E Woods[2002]. Digital Image Processing, 2nd ed, Prentice Hall, Upper Saddle River, NJ.
2) Image Processing Toolbox, Users Guide, Version 4. [2003], The Math works, Inc., Natick, MA.
3) Rafael C Gonzalez, Richard E Woods, Steven L. Eddins [2005].Digital Image Processing using MATLAB,2nd ed, Pearson Education, Singapore
4) [http: texture-review] is available at http://www.cs.iupui.edu/~tuceryan /research/ ComputerVision /texture-review.pdf
5) [http:Computed_tomography] is available at http://en.wikipedia. org/wiki/ Computed_to mography
6) [http: radiology] is available at http://www.radiology info.org/en /info. cfm?pg=bodyct&bhcp=1
7) [http: Feature_extraction] is available at http://en.wikipedia.org/wiki/ Feature_extraction
8) [http: texture] is available at http://graphics.stanford.edu/projects/texture/
9) [http: matlab] is available at http://www.mathworks.com/products/matlab/
10) [http: advantages] is available at www.medindia.net/patients/patientinfo /CT_Scan_advantages.htm
11) [http: history] is available at http://imaginis.com/ct-scan/history.asp
12) [http: ct] is available at www.lymphomainfo.net/tests/ct.html